Error Analysis of Finite Difference Scheme for American Option Pricing under Regime-Switching with Jumps

Cunxin Huang[a], Haiming Song*[a], Jinda Yang†[b], and Bocheng Zhou[c]

[a] *School of Mathematics, Jilin University, Changchun, 130012, China.*
[b] *School of Science and Engineering, the Chinese University of Hong Kong, Shenzhen, Guangdong, 518172, China; University of Science and Technology of China, Hefei, Anhui, 230026, China.*
[c] *Dornsife College of Letters, Arts and Sciences, University of Southern California, Los Angeles, California, 90007, USA.*

Abstract

This paper mainly focuses on evaluating American options under regime-switching jump-diffusion models (Merton's and Kou's models). An efficient numerical method is designed for the concerned problems. The problem of American option pricing under regime-switching jump-diffusion models can be described as a free-boundary problem or a complementarity problem with integral and differential terms on an unbounded domain. By analyzing the relation of optimal exercise boundaries among several options, we truncate the solving domain of regime-switching jump-diffusion options, and present reasonable boundary conditions. For the integral terms of the truncated model, a composite trapezoidal formula is applied, which guarantees that the integral discretized matrix is a Toeplitz matrix. Meanwhile, a finite difference scheme is proposed for the resulting system, which leads to a linear complementary problem (LCP) with a unique solution. Moreover, we also prove the stability, monotonicity, and consistency of the discretization scheme and estimate the convergence order. In consideration of the characteristics of the discrete matrix, a projection and contraction method is suggested to solve the discretized LCP. Numerical experiments are carried out to verify the efficiency of the proposed scheme.

Keywords American option, regime-switching, jump-diffusion, finite difference method, projection and contraction method.

Mathematics Subject Classification 90C30, 90C33, 65N30

1 Introduction

An option is a financial derivative that allows the holder to buy or sell a specific quantity and quality of underlying assets at a fixed price on a specified date or within an agreed period. In options trading, the fixed price is called the strike price, and the fixed date is called the expiration date. According to the difference between buying and selling the underlying asset in the contract, options can be divided into call options (buy) and put options (sell). According to the different execution times of the option, it can also be divided into European

*Corresponding Author: songhaiming@jlu.edu.cn (H. Song)
†Corresponding Author: yangjinda@cuhk.edu.cn (J. Yang)

options and American options. European options must be implemented on the expiration date specified in the contract, while American options can be executed on any trading day (including the expiration date) before the expiration date. The option has always been popular because of its characteristics of avoiding the risk of asset price fluctuations and becoming a critical hedging tool.

As the financial market takes off, the option pricing problem has been paid more and more attention by issuing companies and investors. It has become a widespread research problem in financial mathematics. As early as 1900, Bachelier mentioned option pricing in his dissertation [4]. In 1973, Black and Scholes established the famous Black-Scholes model (B-S model) and gave the formula of European option pricing [7]. Since there is no explicit expression for American options, researchers have to resort to numerical methods. Cox et al. proposed the binary tree method [12] in 1979, Han et al. proposed the method based on non-local boundary conditions [18] in 2003, and Yang et al. proposed the front-fixing finite element method [21] in 2008.

To make up for the fact that the classical B-S model can not explain the phenomenon that asset prices jump due to external factors, Merton introduced the Poisson process to describe the fluctuation behavior of asset prices in 1976 [28]. Since then, researchers have begun to study the option pricing model under the jump-diffusion model. Since the model contains a non-local integral term, people prefer a numerical solution to the model. In 2005, Achdou et al. summarized most numerical solutions in their book [1]. Besides, Cont et al. proposed the explicit-implicit finite difference method [10], and Ascher et al. [3] and Frank et al. [15] designed a second-order explicit-implicit method.

Over the past few decades, researchers found that standard option pricing models cannot accurately account for cyclical changes in option prices caused by short-term political or economic uncertainty. In 1989, Hamilton first proposed the regime-switching model for American option pricing [17]. In 2002, the research results of Elliot and Buffington made the model more popular [8]. In addition to option pricing, researchers also generalized the regime-switching model to other fields [13, 16, 19, 37]. Numerous research work on numerical methods of option pricing under the regime-switching model can refer to [9, 24, 33, 36].

Inherently, researchers try combining the regime-switching and jump-diffusion models in American option pricing. The main task of this problem is to solve a system of coupled partial integro-differential equations (PIDEs), and it is difficult to obtain a closed-form solution. Hence, researchers used several numerical methods to get its numerical solution in recent years. Lee designed a second-order finite difference method [27]. Bastani et al. used a radial basis collocation method in a meshfree framework [6]. More recent related works can refer to [23, 29, 31, 32, 34, 35].

The problem of American option pricing under regime-switching jump-diffusion models poses two main challenges for efficient numerical implementation. The first challenge is that this problem has an infinite domain, and a reasonable truncation should be given to localize it. In our work, we propose a novelty truncation technique for solving American options on a bounded domain. The truncated condition is accurate on the left and relaxed on the right, where the looseness is admissible because the option price tends to zero on the right. Our new truncation technique also could avoid part of the numerical error since some integral terms can be calculated precisely in the pricing model. The second challenge is that it is difficult to conceive a succinct numerical scheme with complete theoretical analysis and efficient numerical solutions for evaluating options. By our truncation tactic, the standard composite trapezoidal formula and finite difference scheme are competent for the discretization of the truncated model problem and result in a discretized LCP, which has a numerically friendly structure and can be solved effectively by projection and contraction method (PCM). We analyze the stability, monotonicity, and consistency of the discretization scheme, and establish the error estimation additionally. The numerical experiments show the efficiency of our method for Merton's and Kou's models. To our knowledge, this paper's work on truncation technique and numerical analysis is unexplored for the PIDE-LCP model arising from American option pricing under regime-switching with jumps.

The rest of this paper is organized as follows. In Section 2, we introduce the original option pricing model and its simplified form, respectively. We also use truncation techniques to localize the infinite domain of the simplified pricing model to be a bounded one. The discretized model is presented by applying the composite trapezoidal formula and finite difference method in Section 3. Simultaneously, we analyze the related properties of the discretization scheme and estimate the convergence error. In Section 4, we apply the tailored projection and contraction method to solve the discrete model, and show some convincing numerical results. Conclusions are given in Section 5.

2 Pricing Model and Truncation

In this section, we will briefly describe the mathematical model of American option pricing under regime-switching jump-diffusion models and simplify the model by variable substitutions. Then we propose a truncation technique, which leads to an exact condition on the left boundary.

2.1 Option Pricing Model

Before introducing the pricing model, let us present some preliminary. Suppose α_t is a continuous Markov chain defined in probability space $(\Omega, \mathcal{F}, \mathcal{P})$ and its finite state space is $\mathcal{M} = \{1, 2, \ldots, \mathcal{Q}\}$, where $\mathcal{Q}$ is the total number of states and each state represents a specific regime. According to the Markov chain theory, assume $\mathcal{A} = (\alpha_{ij})_{\mathcal{Q}\times\mathcal{Q}}$ is the generator matrix of α_t, where α_{ij} satisfies the following conditions:

- $\alpha_{ij} \geqslant 0,\ \forall\ i \neq j,\ 1 \leqslant i,\ j \leqslant \mathcal{Q}$;
- $\alpha_{ii} \leqslant 0$ and $\alpha_{ii} = -\sum\limits_{j\neq i} \alpha_{ij},\ 1 \leqslant i \leqslant \mathcal{Q}$.

Under the risk-neutral measure, the underlying asset price S_t satisfies the following stochastic differential equation [27]:

$$\frac{\mathrm{d}S_t}{S_{t-}} = (r_{\alpha_t} - d_{\alpha_t} - \lambda_{\alpha_t}\kappa)\,\mathrm{d}t + \sigma_{\alpha_t}\mathrm{d}\mathcal{W}_t + y_{\alpha_t}\mathrm{d}\mathcal{N}_t^{\alpha_t}, \tag{1}$$

where r_{α_t} is risk-free rate, d_{α_t} and σ_{α_t} stand for the dividend and the volatility of the underlying asset in regime α_t, respectively. $\mathcal{W}_t$ is a Brownian motion and $\mathcal{N}_t^{\alpha_t}$ denotes a Poisson process with intensity λ_{α_t} depending on the regime α_t. y_{α_t} is a set of independent, identically distributed random variables with probability density $g(y)$ and represents the jump amplitude from S_{t-} to S_t in regime α_t. The expected jump percentage is $\kappa = \mathbb{E}\,(y_{\alpha_t} - 1)$. It's worth noting that the stochastic process α_t, $\mathcal{W}_t$, $\mathcal{N}_t^1, \mathcal{N}_t^2, \ldots, \mathcal{N}_t^{\mathcal{Q}}$ are mutually independent.

According to Theorem 6.2 in [22], if we know the price of either an American call option or an American put option, we can calculate the price of the other one directly. Thus, we consider American regime-switching jump-diffusion options on the asset price $S_t = S$, and take the put option with the expiry date T and strike price K as an example. According to the definition of American put option, the solving domain $[0, +\infty) \times [0, T]$ could be divided into holding domain $\Sigma_1^{(i)}$ and exercising domain $\Sigma_2^{(i)}$ in regime i, where $i \in \{1, 2, \dots, \mathcal{Q}\}$. In the holding domain $\Sigma_1^{(i)}$, the option price satisfies $P_i(S,t) > \max\{K - S, 0\}$; and in the exercising domain $\Sigma_2^{(i)}$, the option price satisfies $P_i(S,t) = \max\{K - S, 0\}$. It is not hard to find that there is a natural continuous boundary $\Gamma_i : S = B_i(t),\ 0 \le t \le T$ between $\Sigma_1^{(i)}$ and $\Sigma_2^{(i)}$, which is called optimal exercise boundary.

Based on the stochastic differential equation (1), using $\Delta-$hedge principle and Itô formula, we could derive that the option price $P_i = P_i(S,t)$ on $\Sigma_1^{(i)}$ satisfies the following partial integro-differential equations [14]:

$$
\begin{aligned}
\mathcal{L}_i P_i(S,t) = {} & \frac{\partial P_i}{\partial t} + \frac{1}{2}\sigma_i^2 S^2 \frac{\partial^2 P_i}{\partial S^2} + (r_i - d_i - \lambda_i \kappa)\, S \frac{\partial P_i}{\partial S} \\
& - (r_i + \lambda_i - \alpha_{ii})\, P_i + \sum_{l \neq i} \alpha_{il} P_l + \lambda_i \int_0^{+\infty} P_i\,(Sy, t)\, g\,(y)\, \mathrm{d}y = 0, \quad i = 1, \cdots, \mathcal{Q}.
\end{aligned} \tag{2}
$$

Let $\boldsymbol{P}(S,t) = (P_1(S,t), \dots, P_{\mathcal{Q}}(S,t))^\top$, then the option pricing problem could be described in the form of a set of free boundary problems:

$$
\begin{cases}
\mathcal{L}_i P_i(S,t) = 0, & B_i(t) < S < +\infty, \quad 0 \le t < T, \\
P_i(S,T) = P^*(S), & B_i(T) < S < +\infty, \\
P_i(S,t) = P^*(S), & 0 \le S \le B_i(t), \quad 0 \le t \le T, \\
\dfrac{\partial P_i}{\partial S}\,(B_i(t), t) = -1, & 0 \le t < T, \\
\lim\limits_{S \to +\infty} P_i(S,t) = 0, & 0 \le t < T,
\end{cases} \tag{3}
$$

for $i \in \{1, 2, \dots, \mathcal{Q}\}$, where $P^*(S) = \max\{K - S, 0\}$. In fact, the free boundary problem (3) also could be rewritten as the complementarity problem [27]:

$$
\begin{cases}
-\mathcal{L}_i P_i(S,t) \ge 0, \\
P_i(S,t) - P^*(S) \ge 0, \\
\mathcal{L}_i P_i(S,t) \cdot (P_i(S,t) - P_i^*(S)) = 0, \\
P_i(S,T) = P^*(S), \\
P_i(0,t) = K, \\
\lim\limits_{S \to +\infty} P_i(S,t) = 0,
\end{cases} \tag{4}
$$

for $i \in \{1, 2, \dots, \mathcal{Q}\}$, where $(S,t) \in [0, +\infty) \times [0, T)$.

The complementarity problem (4) is a backward variable-coefficient problem, which could be transformed into a foreword constant-coefficient form by using the transformations

$$
\tau = T - t,\ S = e^x,\ V_i(x,\tau) \triangleq P_i(S,t).
$$

For clarity, we take $\mathcal{Q} = 2$ as an example to present the transformed problem given by

$$
\begin{cases}
\mathfrak{L}_i V_i(x,\tau) \ge 0, \\
V_i(x,\tau) - V^*(x) \ge 0, \\
\mathfrak{L}_i V_i(x,\tau) \cdot (V_i(x,\tau) - V^*(x)) = 0, \\
V_i(x,0) = V^*(x), \\
\lim\limits_{x \to -\infty} V_i(x,\tau) = K, \\
\lim\limits_{x \to +\infty} V_i(x,\tau) = 0,
\end{cases} \tag{5}
$$

for $i \in \{1,2\}$, where $(x,\tau) \in (-\infty,+\infty) \times (0,T]$, $V^*(x) = \max\{K - e^x, 0\}$, and the operator $\mathfrak{L}_i$ is given by

$$\begin{aligned}
\mathfrak{L}_i V_i(x,\tau) = & \frac{\partial V_i}{\partial \tau} - \frac{1}{2}\sigma_i^2 \frac{\partial^2 V_i}{\partial x^2} + \left(\frac{1}{2}\sigma_i^2 - r_i + d_i + \lambda_i \kappa\right) \frac{\partial V_i}{\partial x} \\
& + (r_i + \lambda_i - \alpha_{ii}) V_i - \sum_{l \neq i} \alpha_{il} V_l - \lambda_i \int_0^{+\infty} V_i(x + \ln y, \tau)\, g(y)\, \mathrm{d}y.
\end{aligned} \tag{6}$$

Further, in order to transform the differential part of the operator $\mathfrak{L}_i$ into a conservation form, we make the transformation $V_i(x,\tau) = W_i(x,\tau)e^{\xi_i \tau + \eta_i x}$, where η_i and ξ_i satisfy

$$\begin{cases}
\eta_i = \dfrac{1}{2} + \dfrac{1}{\sigma_i^2}(-r_i + d_i + \lambda_i \kappa), \\
\xi_i = \dfrac{1}{2}\sigma_i^2 \eta_i^2 - (\dfrac{1}{2}\sigma_i^2 - r_i + d_i + \lambda_i \kappa)\eta_i - (r_i + \lambda_i - \alpha_{ii}).
\end{cases}$$

Now, the complementarity problem (5) is simplified to the following form:

$$\begin{cases}
\mathfrak{L}_{c_i} W_i(x,\tau) \geq 0, \\
W_i(x,\tau) - W_i^*(x,\tau) \geq 0, \\
\mathfrak{L}_{c_i} W_i(x,\tau) \cdot (W_i(x,\tau) - W_i^*(x,\tau)) = 0, \\
W_i(x,0) = W_i^*(x,0), \\
\lim\limits_{x \to -\infty} W_i(x,\tau) = \lim\limits_{x \to -\infty} W_i^*(x,\tau), \\
\lim\limits_{x \to +\infty} W_i(x,\tau) = 0,
\end{cases} \tag{7}$$

for all $i \in \{1,2\}$, where $W_i^*(x,\tau) = e^{-\xi_i \tau - \eta_i x} \max\{K - e^x, 0\}$, and the operator $\mathfrak{L}_{c_i}$ is given by

$$\begin{aligned}
\mathfrak{L}_{c_i} W_i(x,\tau) = & \frac{\partial W_i}{\partial \tau} - \frac{1}{2}\sigma_i^2 \frac{\partial^2 W_i}{\partial x^2} - \sum_{l \neq i} \alpha_{il} W_l e^{(\xi_l - \xi_i)\tau + (\eta_l - \eta_i)x} \\
& - \lambda_i \int_0^{+\infty} W_i(x + \ln y, \tau)\, g(y)\, y^{\eta_i} \mathrm{d}y.
\end{aligned}$$

It is necessary to claim that we will specifically consider two different jump-diffusion models: Merton's model [28] and Kou's model [25]. The probability density function in Merton's model can be written as

$$g(y) = \frac{1}{\sqrt{2\pi}\delta y} e^{-\frac{(\ln y - \mu)^2}{2\delta^2}}, \quad \text{(log-normal distribution)}$$

and in Kou's model can be read as

$$g(y) = q\theta_2 y^{\theta_2 - 1} \mathbb{1}_{\{0 \leq y < 1\}} + p\theta_1 y^{-\theta_1 - 1} \mathbb{1}_{\{y \geq 1\}}, \quad \text{(log-double-exponential distribution)}$$

where $\mathbb{1}_\chi$ is the indicator function of the set χ. Note that the parameters μ and δ in log-normal distribution stand for the expectation and standard deviation of the random variable $\ln y$, respectively. And the parameters in log-double-exponential distribution must satisfy that $p, q, \theta_2 > 0$, $\theta_1 > 1$, and $p + q = 1$.

2.2 Truncation technique

In this subsection, we will introduce a truncation technique to truncate the infinite spatial domain of the simplified model (7) into a bounded one. The technique consists of an exact truncation on the left and an empirical estimation truncation on the right. We discuss the original problem (3) before transformations, and establish inequalities of prices and optimal exercise boundaries between the original problem and its two related problems firstly. Then, with the help of the inequalities, the left boundary of the solution domain in (7) shall be truncated at a fixed position, and an exact boundary condition is obtained.

For clearness, we first review the following two types of options.

Definition 1. *An option is called a permanent American put option under jump-diffusion model in regime i ($i = 1, 2, \dots, \mathcal{Q}$) if its value function $\bar{P}_i = \bar{P}_i(S)$ satisfies*

$$\begin{cases} \bar{\mathcal{L}}_i \bar{P}_i(S) = 0, \quad \bar{B}_i < S < +\infty, \\ \dfrac{\partial \bar{P}_i}{\partial S}(\bar{B}_i) = -1, \\ \bar{P}_i(\bar{B}_i) = K - \bar{B}_i, \\ \lim\limits_{S \to +\infty} \bar{P}_i(S) = 0, \end{cases} \tag{8}$$

where $\bar{B}_i$ is the optimal exercise boundary, and the operator $\bar{\mathcal{L}}_i$ is given as:

$$\bar{\mathcal{L}}_i \bar{P}_i = \frac{1}{2}\sigma_i^2 S^2 \frac{\mathrm{d}^2 \bar{P}_i}{\mathrm{d}S^2} + (r_i - d_i - \lambda_i \kappa) S \frac{\mathrm{d}\bar{P}_i}{\mathrm{d}S} - (r_i + \lambda_i)\bar{P}_i + \lambda_i \int_0^{+\infty} \bar{P}_i(Sy) g(y) \mathrm{d}y.$$

Definition 2. *An option is called an American put option under jump-diffusion model in regime i ($i = 1, 2, \dots, \mathcal{Q}$) if its value function $\tilde{P}_i = \tilde{P}_i(S, t)$ satisfies*

$$\begin{cases} \tilde{\mathcal{L}}_i \tilde{P}_i(S,t) = 0, & \tilde{B}_i(t) < S < +\infty, \quad 0 \le t < T, \\ \tilde{P}_i(S,t) = \max\{K - S, 0\}, & 0 \le S \le \tilde{B}_i(t), \quad 0 \le t \le T, \\ \tilde{P}_i(S,T) = \max\{K - S, 0\}, & \tilde{B}_i(T) < S < +\infty, \\ \dfrac{\partial \tilde{P}_i}{\partial S}\left(\tilde{B}_i(t), t\right) = -1, & 0 \le t < T, \\ \lim\limits_{S \to +\infty} \tilde{P}_i(S,t) = 0, & 0 \le t < T, \end{cases} \tag{9}$$

where $\tilde{B}_i(t)$ is the optimal exercise boundary, and the operator $\tilde{\mathcal{L}}_i$ is given as:

$$\tilde{\mathcal{L}}_i \tilde{P}_i = \frac{\partial \tilde{P}_i}{\partial t} + \frac{1}{2}\sigma_i^2 S^2 \frac{\partial^2 \tilde{P}_i}{\partial S^2} + (r_i - d_i - \lambda_i \kappa) S \frac{\partial \tilde{P}_i}{\partial S} - (r_i + \lambda_i)\tilde{P}_i + \lambda_i \int_0^{+\infty} \tilde{P}(Sy, t) g(y) \mathrm{d}y.$$

Next, we recall some useful results by the following lemmas, which helps us establish inequalities of prices and optimal exercise boundaries between the original problem and its two related problems.

Lemma 1 (cf. [30])**.** *The option price $\tilde{P}_i(S, t)$ decreases monotonically with respect to S and t. And the optimal exercise boundary $\tilde{B}_i(t)$ increases monotonically with respect to t, which leads to*

$$\tilde{B}_i(t) \le \tilde{B}_i(T) = K \min\left\{\frac{r_i}{d_i},\ 1\right\}. \tag{10}$$

Here, $\tilde{P}_i(S, t)$ and $\tilde{B}_i(t)$ are defined in Definition 2.

Lemma 2 (cf. [30])**.** *If $T_1 \geq T_2$ and $t \in [0, T_2]$, we have*

$$\begin{aligned} &\tilde{P}_i(S,t;T_2) \leq \tilde{P}_i(S,t;T_1) \leq \tilde{P}_i(S,t;\infty) = \bar{P}_i(S), \\ &\bar{B}_i = \tilde{B}_i(t;\infty) \leq \tilde{B}_i(t;T_1) \leq \tilde{B}_i(t;T_2), \end{aligned} \tag{11}$$

where $\tilde{P}_i(S,t;T)$ represents the option price defined in Definition 2 with expiry date T, and $\tilde{B}_i(t;T)$ is the same. In addition, $\bar{P}_i(S)$ and $\bar{B}_i$ are defined in Definition 1.

Lemma 3 (cf. [30])**.** *For all $t \in [0, T)$, $\tilde{P}_i(S,t)$ is a convex function respect to S, so we have*

$$\frac{\partial^2 \tilde{P}_i}{\partial S^2}(S,t) \geq 0,$$

where $\tilde{P}_i(S,t)$ is defined in Definition 2.

Now, we can obtain the following inequalities for option prices and optimal exercise boundaries.

Theorem 1. *Suppose that $\mathcal{Q} = 2$ in problem (3), and $r_1 = r_2$, $d_1 = d_2$, $\sigma_1 \geq \sigma_2$, $\lambda_1 \geq \lambda_2$, then we have*

$$\begin{aligned} &P_i(S,t) \leq \tilde{P}_1(S,t) \leq \bar{P}_1(S), \\ &\bar{B}_1 \leq \tilde{B}_1(t) \leq B_i(t), \end{aligned} \tag{12}$$

where $\bar{P}_1(S)$ and $\bar{B}_1$ are defined in Definition 1, $\tilde{P}_1(S,t)$ and $\tilde{B}_1(t)$ are defined in Definition 2, and $P_i(S,t)$ and $B_i(t)$ are the option price and optimal exercise boundary for American put options under the regime-switching jump-diffusion models with $i = 1, 2$.

Proof. We only need to prove the inequalities of option prices, and the inequalities of optimal exercise boundaries will be obtained once those of option prices are achieved.

Let $\boldsymbol{P}(S,t) = (\tilde{P}_1(S,t), \tilde{P}_1(S,t))^\top$. Using the definition of $\tilde{\mathcal{L}}_1$ and the property that $\tilde{\mathcal{L}}_1 \tilde{P}_1 \leq 0$, we can obtain that

$$\mathcal{L}_1 \tilde{P}_1 = \tilde{\mathcal{L}}_1 \tilde{P}_1 + (\alpha_{11} + \alpha_{12}) \tilde{P}_1 \leq 0. \tag{13}$$

By the assumptions $r_1 = r_2$, $d_1 = d_2$, and $\sigma_1 \geq \sigma_2$, we can get

$$\begin{aligned} \mathcal{L}_2 \tilde{P}_1 =& \tilde{\mathcal{L}}_1 \tilde{P}_1 + \frac{1}{2}\left(\sigma_2^2 - \sigma_1^2\right) S^2 \frac{\partial \tilde{P}_1^2}{\partial S^2} - (\lambda_2 - \lambda_1)\kappa S \frac{\partial \tilde{P}_1}{\partial S} \\ & - (\lambda_2 - \lambda_1)\tilde{P}_1 + (\lambda_2 - \lambda_1) \int_0^{+\infty} \tilde{P}_1(Sy,t) g(y) \mathrm{d}y \\ \leq& (\lambda_2 - \lambda_1) \int_0^{+\infty} \left(\tilde{P}_1(Sy,t) - \tilde{P}_1(S,t) - (Sy - S)\frac{\partial \tilde{P}_1}{\partial S}(S,t) \right) g(y) \mathrm{d}y. \end{aligned} \tag{14}$$

To be precise, here we use the property of $\tilde{\mathcal{L}}_1 \tilde{P}_1 \leq 0$, the conclusion of Lemma 3, the definition of κ ($\kappa = \mathbb{E}(y-1)$) and the property of probability density functions ($\int_0^{+\infty} g(y) \mathrm{d}y = 1$) in order.

Furthermore, by the convexity of $\tilde{P}_1(\cdot, t)$ (see lemma 3) and $\lambda_1 \geq \lambda_2$, we know the right-hand side of inequality (14) is nonpositive. Moreover, it is not difficult to find that the inequality $P_i \leq \tilde{P}_1$ always holds in the boundary without considering the position of the optimal exercise boundaries. Therefore, we can use the comparison principle [14] to obtain the left price inequality. The right inequality of prices is already given by Lemma 2. □

Remark 1. We notice that $\bar{B}_1$ in Theorem 1 is determined by the density function $g(y)$. In specific, if we choose Merton's model, we can obtain that $\bar{B}_i = K\beta/(\beta-1)$, where β is the negative root of the equation

$$G(x) = \frac{1}{2}\sigma_i^2 x^2 + (r_i - d_i - \lambda_i \kappa - \frac{1}{2}\sigma_i^2)x - (r_i + \lambda_i) + \lambda_i e^{\mu x + \frac{1}{2}\delta^2 x} = 0.$$

If we choose Kou's model, we can obtain that $\bar{B}_i = K(\theta_2+1)\gamma_1\gamma_2/(\theta_2(\gamma_1-1)(\gamma_2-1))$, where $\gamma_1 > \gamma_2$, and they both are the negative roots of the equation

$$G(x) = \frac{1}{2}\sigma_i^2 x^2 + \left(r_i - d_i - \lambda_i \kappa - \frac{1}{2}\sigma_i^2\right)x - (r_i + \lambda_i) + \lambda_i \left(\frac{q\theta_2}{\theta_2 + x} + \frac{p\theta_1}{\theta_1 - x}\right) = 0.$$

Since the values of $\bar{B}_i$ have been given both in Merton's model and Kou's model, by Theorem 1, we can directly use $\min\{\bar{B}_1, \bar{B}_2\}$ as the left truncation location of the problem (3), and obtain an exact left boundary condition with the payoff form. Naturally, $\ln\min\{\bar{B}_1, \bar{B}_2\}$ shall be applied as the left truncation location of the problem (7) with an exact boundary condition. For the empirical truncation estimation on the right of the problem (7), it has been shown that the error caused by the right-hand truncation decreases exponentially pointwise with respect to $\ln S$. Similarly, we choose $L_0 = \ln 3K$ as the right-hand truncation boundary [10], and the corresponding right boundary condition is set to zero.

Combining the truncations of both sides, we truncate the infinite domain $\mathbb{R}$ to be $[-L, L]$, where $L = \max\{-\ln\min\{\bar{B}_1, \bar{B}_2\}, L_0\}$. Therefore, we have the option pricing model on a bounded domain as follows:

$$\begin{cases} \mathscr{L}_i w_i(x,\tau) \geq 0, \\ w_i(x,\tau) - w_i^*(x,\tau) \geq 0, \\ \mathscr{L}_i w_i(x,\tau) \cdot (w_i(x,\tau) - w_i^*(x,\tau)) = 0, \\ w_i(x,0) = w_i^*(x,0), \\ w_i(-L,\tau) = w_i^*(-L,\tau), \\ w_i(L,\tau) = 0, \end{cases} \tag{15}$$

for $i \in \{1,2\}$, where $(x,\tau) \in (-L,L)\times(0,T]$, $w_i^*(x,\tau) = e^{-\xi_i\tau - \eta_i x}\max\{K - e^x, 0\}$, and the operator $\mathscr{L}_i$ is given by:

$$\begin{aligned} \mathscr{L}_i w_i(x,\tau) =& \frac{\partial w_i}{\partial \tau} - \frac{1}{2}\sigma_i^2 \frac{\partial^2 w_i}{\partial x^2} - \alpha_{il} w_l e^{(\xi_l - \xi_i)\tau + (\eta_l - \eta_i)x} \\ & - \lambda_i \int_0^{e^{L-x}} w_i\left(x + \ln y, \tau\right) g\left(y\right) y^{\eta_i} \mathrm{d}y, \quad l = 3 - i. \end{aligned} \tag{16}$$

Remark 2. Although Theorem 1 is only proved under the assumption that $r_1 = r_2$ and $d_1 = d_2$, we can also use this truncation technique in more general cases since the optimal exercise boundary of permanent American option can guarantee the accuracy of the left-hand side truncation and $\ln 3K$ provides a safeguard for the left-hand side truncation.

3 Numerical Discretization and Error Estimation

In this section, we will discuss the discretization of the option pricing problem (15) and analyze some properties of the discretization scheme. Also, we will establish the corresponding error estimation in the last subsection.

3.1 Discretized LCP

For numerical implementation, a composite trapezoidal formula and a finite difference method will be used to deal with the integral term and differential terms in the operator $\mathscr{L}_i$, respectively. Then, we will obtain a linear complementarity problem in finite dimension.

We advance some notations. Let J_τ and I_h stand for the temporal and spatial partition, respectively. Specifically,

$$
\begin{aligned}
&J_\tau : 0 = \tau_0 < \tau_1 < \cdots < \tau_{N_t} = T, \\
&\Delta\tau = \frac{T}{N_t}, \quad \tau_n = \tau_0 + n\Delta\tau, \quad n = 0, 1, \cdots, N_t, \\
&I_h : -L = x_0 < x_1 < \cdots < x_{N_x} = L, \\
&\Delta x = \frac{2L}{N_x}, \quad x_j = x_0 + j\Delta x, \quad j = 0, 1, \cdots, N_x.
\end{aligned}
\tag{17}
$$

We use $w_{i,j}^n$ for the function value of $w_i(x_j, \tau_n)$, which is the exact solution of (15) at the partition node (x_j, τ_n), where $i = 1, 2$, $j = 0, 1, \ldots, N_x$, and $n = 0, 1, \ldots, N_t$. We also utilize $u_{i,j}^n$ for the numerical solution in subsequence, which is the approximation of $w_{i,j}^n$.

Considering the challenge of dealing with the integral term in $\mathscr{L}_i$, we design its discretization scheme first. In the case of Merton's model, changing the variable $\ln y$ to z, the integral term

$$
I_i(x, \tau) = \int_0^{e^{L-x}} w_i\left(x + \ln y, \tau\right) g\left(y\right) y^{\eta_i} \mathrm{d}y, \tag{18}
$$

could be rewritten as

$$
I_i(x, \tau) = C_i \int_{-\infty}^{L-x} w_i\left(x + z, \tau\right) e^{-\frac{(z-\mu_i^*)^2}{2\delta^2}} \mathrm{d}z,
$$

where $C_i = e^{(\mu\eta_i - \frac{1}{2}\delta^2\eta_i^2)}/(\delta\sqrt{2\pi})$ and $\mu_i^* = \mu + \delta^2\eta_i$. In addition, we use the composite trapezoidal formula to approximate $I_i(x, \tau)$ at the point (x_j, τ_n) as follows,

$$
\begin{aligned}
I_i(x_j, \tau_n) &= C_i \sum_{k=0}^{N_x-1} \int_{(k-j)\Delta x}^{(k-j+1)\Delta x} w_i(x_j + z, \tau_n) e^{-\frac{(z-\mu_i^*)^2}{2\delta^2}} \mathrm{d}z \\
&\quad + C_i \int_{-\infty}^{-j\Delta x} w_i^*(x_j + z, \tau_n) e^{-\frac{(z-\mu_i^*)^2}{2\delta^2}} \mathrm{d}z \\
&\approx \frac{C_i \Delta x}{2} \sum_{k=0}^{N_x-1} \left[u_{i,k}^n e^{-\frac{((k-j)\Delta x - \mu_i^*)^2}{2\delta^2}} + u_{i,k+1}^n e^{-\frac{((k-j+1)\Delta x - \mu_i^*)^2}{2\delta^2}} \right] + \boldsymbol{R}_{i,j}^n \\
&= \frac{C_i \Delta x}{2} \boldsymbol{\Phi}_{i,j}^\top \boldsymbol{U}_i^n + \boldsymbol{R}_{i,j}^n,
\end{aligned}
\tag{19}
$$

where

$$
\begin{aligned}
&\boldsymbol{\Phi}_{i,j} = \left(\phi_{i,j,0}, 2\phi_{i,j,1}, \cdots, 2\phi_{i,j,N_x-1}, \phi_{i,j,N_x}\right)^\top, \\
&\phi_{i,j,k} = e^{-\frac{((k-j)\Delta x - \mu_i^*)^2}{2\delta^2}}, \quad k = 0, 1, \cdots, N_x, \\
&\boldsymbol{U}_i^n = \left(u_{i,0}^n, u_{i,1}^n, \ldots, u_{i,N_x}^n\right)^\top, \\
&\boldsymbol{R}_{i,j}^n = C_i \int_{-\infty}^{-j\Delta x} w_i^*(x_j + z, \tau_n) e^{-\frac{(z-\mu_i^*)^2}{2\delta^2}} \mathrm{d}z.
\end{aligned}
$$

In particular, $\boldsymbol{R}_{i,j}^n$ can be written as

$$\boldsymbol{R}_{i,j}^n = e^{-\eta_i(-L+j\Delta x)-\xi_i\tau_n}\left(Ke^{-\delta^2\eta_i^2}N_{\mu,\delta^2}(-j\Delta x) - e^{\mu+\frac{1}{2}\delta^2-L+j\Delta x-\delta^2\eta_i^2}N_{\mu+\delta^2,\delta^2}(-j\Delta x)\right),$$

where $N_{a,b^2}(x)$ represents the cumulative distribution function of normal distribution with mean a and variance b^2.

In the case of Kou's model, we employ the same variable substitution as for Merton's model and have the following approximation,

$$\begin{aligned}
I_i(x_j,\tau_n) &= q\theta_2\sum_{k=0}^{j-1}\int_{(k-j)\Delta x}^{(k-j+1)\Delta x} w_i\left(x_j+z,\tau_n\right)e^{(\eta_i+\theta_2)z}\mathrm{d}z \\
&\quad + p\theta_1\sum_{k=j}^{N_x-1}\int_{(k-j)\Delta x}^{(k-j+1)\Delta x} w_i\left(x_j+z,\tau_n\right)e^{(\eta_i-\theta_1)z}\mathrm{d}z \\
&\quad + q\theta_2\int_{-\infty}^{-j\Delta x} w_i^*\left(x_j+z,\tau_n\right)e^{(\eta_i+\theta_2)z}\mathrm{d}z \\
&\approx \frac{Q\Delta x}{2}\sum_{k=0}^{j-1}\left[e_{i,j,k}^Q u_{i,k}^n + e_{i,j,k+1}^Q u_{i,k+1}^n\right] \\
&\quad + \frac{P\Delta x}{2}\sum_{k=j}^{N_x-1}\left[e_{i,j,k}^P u_{i,k}^n + e_{i,j,k+1}^P u_{i,k+1}^n\right] + \boldsymbol{R}_{i,j}^n \\
&= \frac{C_i\Delta x}{2}\boldsymbol{\Phi}_{i,j}^\top\boldsymbol{U}_i^n + \boldsymbol{R}_{i,j}^n,
\end{aligned} \tag{20}$$

where $C_i = 1$,

$$\begin{aligned}
Q &= q\theta_2, \qquad e_{i,j,k}^Q = e^{((\eta_i+\theta_2)(k-j)\Delta x)}, \\
P &= p\theta_1, \qquad e_{i,j,k}^P = e^{((\eta_i+\theta_1)(k-j)\Delta x)}, \\
\boldsymbol{\Phi}_{i,j} &= \Big[Qe_{i,j,0}^Q, 2Qe_{i,j,1}^Q, \ldots, 2Qe_{i,j,j-1}^Q, \\
&\quad \left(Qe_{i,j,j}^Q + Pe_{i,j,j}^P\right), 2Pe_{i,j,j+1}^P, \ldots, 2Pe_{i,j,N_x-1}^P, Pe_{i,j,N_x}^P\Big]^\top, \\
\boldsymbol{R}_{i,j}^n &= q\theta_2\int_{-\infty}^{-j\Delta x} w_i^*\left(x_j+z,\tau_n\right)e^{(\eta_i+\theta_2)z}\mathrm{d}z.
\end{aligned}$$

Specifically, we can compute $\boldsymbol{R}_{i,j}^n$ by

$$\boldsymbol{R}_{i,j}^n = qe^{\eta_i L-\eta_i j\Delta x-\theta_2 j\Delta x-\xi_i\tau_n}\left(K - \frac{\theta_2}{1+\theta_2}e^{-L}\right).$$

It needs to notice that the values of the vector $\boldsymbol{\Phi}_{i,j}$, C_i and $\boldsymbol{R}_{i,j}^n$ in (19) and (20) are different, and we write them in an invariant form for the subsequent analysis.

Now, we consider approximating the differential terms, which will be discretized by the backward Euler method in the temporal direction and central difference quotient for the second-order partial derivative in the spatial direction as follows,

$$\begin{aligned}
\frac{\partial w_i}{\partial\tau}(x_j,\tau_{n+1}) &\approx \frac{u_{i,j}^{n+1}-u_{i,j}^n}{\Delta\tau}, \\
\frac{\partial^2 w_i}{\partial x^2}(x_j,\tau_{n+1}) &\approx \frac{u_{i,j+1}^{n+1}-2u_{i,j}^{n+1}+u_{i,j-1}^{n+1}}{(\Delta x)^2}.
\end{aligned}$$

Based on the above approximations of the integral term and differential terms, we now present the discretization of the option pricing problem (15) in point-by-point form, which can be read as

$$\begin{cases} \boldsymbol{L}_i u_{i,j}^{n+1} \geq 0, \\ u_{i,j}^{n+1} - u_{i,j}^{n+1,*} \geq 0, \\ \boldsymbol{L}_i u_{i,j}^{n+1} \cdot (u_{i,j}^{n+1} - u_{i,j}^{n+1,*}) = 0, \\ u_{i,j}^{0} = u_{i,j}^{0,*}, \\ u_{i,0}^{n} = u_{i,0}^{n,*}, \\ u_{i,N_x}^{n} = 0, \end{cases} \tag{21}$$

for $i = 1, 2$, and any fixed (j, n), $j = 1, 2, \ldots, N_x - 1$, $n = 0, 1, \ldots, N_t - 1$, where $u_{i,j}^{n,*} = e^{-\xi_i \tau_n - \eta_i x_j} \max\{K - e^{x_j}, 0\}$, and the operator $\boldsymbol{L}_i$ is given by:

$$\begin{aligned} \boldsymbol{L}_i u_{i,j}^{n+1} = {} & \frac{u_{i,j}^{n+1} - u_{i,j}^{n}}{\Delta \tau} - \frac{1}{2}\sigma_i^2 \frac{u_{i,j+1}^{n+1} - 2u_{i,j}^{n+1} + u_{i,j-1}^{n+1}}{(\Delta x)^2} \\ & - \alpha_{il} e^{((\xi_l - \xi_i)\tau_n + (\eta_l - \eta_i)x_j)} u_{l,j}^{n} - \lambda_i \left(\frac{C_i \Delta x}{2} \boldsymbol{\Phi}_{i,j}^{\top} \boldsymbol{U}_i^n + \boldsymbol{R}_{i,j}^n \right), \quad l = 3 - i. \end{aligned} \tag{22}$$

Since the value at the boundary is known, for simplicity we denote the vector to be solved in terms of $\bar{\boldsymbol{U}}^n = (\bar{\boldsymbol{U}}_1^n; \bar{\boldsymbol{U}}_2^n)$, where

$$\bar{\boldsymbol{U}}_i^n = \left(u_{i,1}^n, u_{i,2}^n, \ldots, u_{i,N_x-1}^n\right)^{\top}, \qquad i = 1, 2.$$

We should pay attention that $\boldsymbol{U}^n = (\boldsymbol{U}_1^n; \boldsymbol{U}_2^n)$ is a $2(N_x + 1)$-dimensional vector while $\bar{\boldsymbol{U}}^n = (\bar{\boldsymbol{U}}_1^n; \bar{\boldsymbol{U}}_2^n)$ is a $2(N_x - 1)$-dimensional vector.

Furthermore, let

$$\begin{aligned} & \bar{\boldsymbol{U}}^{n,*} = \left(\bar{\boldsymbol{U}}_1^{n,*}; \bar{\boldsymbol{U}}_2^{n,*}\right) = \left(u_{1,1}^{n,*}, \ldots, u_{1,N_x-1}^{n,*}, u_{2,1}^{n,*}, \ldots, u_{2,N_x-1}^{n,*}\right)^{\top}. \\ & \beta = \Delta\tau/(\Delta x)^2, \quad \rho_i = -\alpha_{il} \Delta\tau e^{-(\eta_l - \eta_i)L + (\xi_l - \xi_i)n\Delta\tau}, \quad i = 1, 2, \quad l = 3 - i, \end{aligned}$$

and we can rewrite the discretized model (21) into a matrix-vector form as follows:

$$\begin{cases} \left(\boldsymbol{A}\bar{\boldsymbol{U}}^n + \boldsymbol{B}\bar{\boldsymbol{U}}^{n+1} - \Delta\tau\boldsymbol{\Phi}\bar{\boldsymbol{U}}^n + \boldsymbol{F}, \bar{\boldsymbol{U}}^{n+1} - \bar{\boldsymbol{U}}^{n+1,*}\right) = 0, \\ \boldsymbol{A}\bar{\boldsymbol{U}}^n + \boldsymbol{B}\bar{\boldsymbol{U}}^{n+1} - \Delta\tau\boldsymbol{\Phi}\bar{\boldsymbol{U}}^n + \boldsymbol{F} \geq 0, \quad \bar{\boldsymbol{U}}^{n+1} - \bar{\boldsymbol{U}}^{n+1,*} \geq 0, \\ \bar{\boldsymbol{U}}^0 = \bar{\boldsymbol{U}}^{0,*}, \end{cases} \tag{23}$$

for $n = 0, 1, \ldots, N_t - 1$, where

$$\boldsymbol{A} = \begin{pmatrix} -\boldsymbol{I} & \boldsymbol{A}_1 \\ \boldsymbol{A}_2 & -\boldsymbol{I} \end{pmatrix}, \quad \boldsymbol{A}_i = \rho_i \cdot \begin{pmatrix} e^{(\eta_l - \eta_i)\Delta x} & & \\ & \ddots & \\ & & e^{(\eta_l - \eta_i)(N_x - 1)\Delta x} \end{pmatrix}_{(N_x-1)\times(N_x-1)},$$

$$\boldsymbol{B} = \begin{pmatrix} \boldsymbol{B}_1 & \boldsymbol{O} \\ \boldsymbol{O} & \boldsymbol{B}_2 \end{pmatrix}, \quad \boldsymbol{B}_i = \begin{pmatrix} 1 + \sigma_i^2\beta & -\frac{\sigma_i^2}{2}\beta & & \\ -\frac{\sigma_i^2}{2}\beta & \ddots & \ddots & \\ & \ddots & \ddots & -\frac{\sigma_i^2}{2}\beta \\ & & -\frac{\sigma_i^2}{2}\beta & 1 + \sigma_i^2\beta \end{pmatrix}_{(N_x-1)\times(N_x-1)},$$

$$\boldsymbol{\Phi} = \begin{pmatrix} \lambda_1\boldsymbol{\Phi}_1 & \boldsymbol{O} \\ \boldsymbol{O} & \lambda_2\boldsymbol{\Phi}_2 \end{pmatrix}, \quad \boldsymbol{\Phi}_i(j, n) = \frac{C_i}{2}\Delta x \boldsymbol{\Phi}_{i,j}(n+1),$$

and the vector $\boldsymbol{F} = \boldsymbol{F}_D - \Delta\tau \boldsymbol{F}_c - \Delta\tau \boldsymbol{F}_I$ with

$$
\begin{aligned}
\boldsymbol{F}_D &= \left(-\frac{\sigma_1^2\beta}{2}u_{1,0}^{n+1}, 0, \ldots, 0, -\frac{\sigma_2^2\beta}{2}u_{2,0}^{n+1}, 0, \cdots, 0\right)^\top, \\
\boldsymbol{F}_c &= \left(\lambda_1 \boldsymbol{R}_{1,1}^n, \ldots, \lambda_1 \boldsymbol{R}_{1,N_x-1}^n, \lambda_2 \boldsymbol{R}_{2,1}^n, \cdots, \lambda_2 \boldsymbol{R}_{2,N_x-1}^n\right)^\top, \\
\boldsymbol{F}_I &= \frac{\Delta x}{2}\left(\lambda_1 C_1 u_{1,0}^n (\boldsymbol{\Phi}_{1,1}(1), \cdots, \boldsymbol{\Phi}_{1,N_x-1}(1)), \lambda_2 C_2 u_{2,0}^n (\boldsymbol{\Phi}_{2,1}(1), \cdots, \boldsymbol{\Phi}_{2,N_x-1}(1))\right)^\top.
\end{aligned}
$$

Let $\mathscr{F}\left(\bar{\boldsymbol{U}}^n\right) = \boldsymbol{A}\bar{\boldsymbol{U}}^n - \Delta\tau \boldsymbol{\Phi}\bar{\boldsymbol{U}}^n + \boldsymbol{F}$, and the problem (23) can be reformulated into the following form:

$$
\begin{cases}
\left(\boldsymbol{B}\bar{\boldsymbol{U}}^{n+1} + \mathscr{F}\left(\bar{\boldsymbol{U}}^n\right), \bar{\boldsymbol{U}}^{n+1} - \bar{\boldsymbol{U}}^{n+1,*}\right) = 0, \\
\boldsymbol{B}\bar{\boldsymbol{U}}^{n+1} + \mathscr{F}\left(\bar{\boldsymbol{U}}^n\right) \geq 0, \quad \bar{\boldsymbol{U}}^{n+1} - \bar{\boldsymbol{U}}^{n+1,*} \geq 0, \\
\bar{\boldsymbol{U}}^0 = \bar{\boldsymbol{U}}^{0,*}.
\end{cases} \tag{24}
$$

Remark 3. It is clear that for given $\bar{\boldsymbol{U}}^n$, the problem (24) is a linear complementarity problem (LCP) with respect to $\bar{\boldsymbol{U}}^{n+1}$. By the definition of the matrix $\boldsymbol{B}$ in (23), it is easy to check $\boldsymbol{B}$ is symmetric and strictly diagonally dominant, and the elements on the diagonal of the matrix $\boldsymbol{B}$ are all positive. Thus, the matrix $\boldsymbol{B}$ is positive definite. Moreover, we can get the uniqueness of the solution of the LCP (24) by the work in [11], which implies the LCP (21) is well posed.

Remark 4. It should be paid attention that our discretized model (24) can be extended to the case where the number of regime is greater than or equal to 3. Suppose we have $\mathcal{Q}$ regimes in our discretized model (24), where $\mathcal{Q} \geq 3$. Then the discretized matrix B will become a $\mathbb{R}^{\mathcal{Q}(N_x-1)\times\mathcal{Q}(N_x-1)}$ matrix and the vector $\bar{\boldsymbol{U}}^n$ will become a $\mathbb{R}^{\mathcal{Q}(N_x-1)\times 1}$ vector. Their specific formulae are as follows

$$
\boldsymbol{B} = \begin{pmatrix} \boldsymbol{B}_1 & & & & \\ & \ddots & & & \\ & & \boldsymbol{B}_i & & \\ & & & \ddots & \\ & & & & \boldsymbol{B}_{\mathcal{Q}} \end{pmatrix}, \quad \boldsymbol{B}_i = \begin{pmatrix} 1+\sigma_i^2\beta & -\frac{\sigma_i^2}{2}\beta & & \\ -\frac{\sigma_i^2}{2}\beta & \ddots & \ddots & \\ & \ddots & \ddots & -\frac{\sigma_i^2}{2}\beta \\ & & -\frac{\sigma_i^2}{2}\beta & 1+\sigma_i^2\beta \end{pmatrix}_{(N_x-1)\times(N_x-1)},
$$

$$
\bar{\boldsymbol{U}}^n = \left(\bar{\boldsymbol{U}}_1^n; \cdots; \bar{\boldsymbol{U}}_i^n; \cdots; \bar{\boldsymbol{U}}_{\mathcal{Q}}^n\right) = \left(u_{1,1}^n, \ldots, u_{1,N_x-1}^n, \cdots, u_{i,1}^n, \ldots, u_{i,N_x-1}^n, \cdots, u_{\mathcal{Q},1}^n, \ldots, u_{\mathcal{Q},N_x-1}^n\right)^\top.
$$

And the corresponding changes to $\mathscr{F}\left(\bar{\boldsymbol{U}}^n\right)$ and $\bar{\boldsymbol{U}}^{n,*}$ are in the same way. In fact, based on the structure of $\boldsymbol{B}$, the discretized model (24) with $\mathcal{Q}$ regimes could be decomposed into $\mathcal{Q}$ subproblems and solve them in parallel. Therefore, the increase in the number of regime will not increase the dimension of the subproblem, which leads to a small increase in computation time.

3.2 Stability, Monotonicity, and Consistency

In this subsection, we will verify the stability, monotonicity, and consistency of the discretization scheme. We first start with the stability analysis.

Theorem 2. *Given the temporal and spatial partitions by (17), the discretized model (21) is stable for initial value, which means that there is a constant C satisfying*

$$
\|\boldsymbol{U}^{n+1}\|_\infty \leq C\|\boldsymbol{U}^0\|_\infty, \ \forall\, n \in \{0, 1, \cdots, N_t - 1\}. \tag{25}
$$

Proof. Let $m = \arg\max_{0\le j\le N_x}\left\{\max\{|u_{1,j}^{n+1}|,|u_{2,j}^{n+1}|\}\right\}$, according to the nonnegativity of $u_{i,j}^{n+1}$, it has $\|\boldsymbol{U}^{n+1}\|_\infty = \max\{u_{1,m}^{n+1}, u_{2,m}^{n+1}\}$. Without loss of generality, we assume $\|\boldsymbol{U}^{n+1}\|_\infty = u_{1,m}^{n+1}$. Observing the discretized model (21), we divide the value of $u_{1,m}^{n+1}$ into two cases to discuss the stability of the numerical scheme.

On the one hand, if $u_{1,m}^{n+1} = u_{1,m}^{n+1,*}$, then

$$
\begin{aligned}
\|\boldsymbol{U}^{n+1}\|_\infty &= u_{1,m}^{n+1,*}\\
&= e^{-\xi_1\tau_{n+1}-\eta_1 x_m}\max\{K-e^{x_m},0\}\\
&= e^{-\xi_1\Delta\tau}e^{-\xi_1\tau_n-\eta_1 x_m}\max\{K-e^{x_m},0\}\\
&= e^{-\xi_1\Delta\tau}u_{1,m}^{n,*}\\
&\le \max\{e^{-\xi_1\Delta\tau}, e^{-\xi_2\Delta\tau}\}u_{1,m}^{n,*}\\
&\le e^{-\xi^*\Delta\tau}\|\boldsymbol{U}^n\|_\infty,
\end{aligned}
\tag{26}
$$

where $\xi^* = \min\{\xi_1,\xi_2\}$.

On the other hand, if $u_{1,m}^{n+1} > u_{1,m}^{n+1,*}$ and satisfies $\boldsymbol{L}_1 u_{i,m}^{n+1} = 0$, by applying the definition of the operator $\boldsymbol{L}_i$ in (22), it has

$$
\begin{aligned}
u_{1,m}^{n+1} - u_{1,m}^{n} - &\frac{1}{2}\sigma_1^2\beta(u_{1,m+1}^{n+1} - 2u_{1,m}^{n+1} + u_{1,m-1}^{n+1}) - \alpha_{12}\Delta\tau e^{((\xi_2-\xi_1)\tau_n+(\eta_2-\eta_1)x_m)}u_{2,m}^{n}\\
&- \lambda_1\Delta\tau\boldsymbol{R}_{1,m}^n - \frac{\lambda_1 C_1\Delta\tau\Delta x}{2}\boldsymbol{\Phi}_{1,m}^\top\boldsymbol{U}_1^n = 0.
\end{aligned}
$$

Then, using the triangle inequality, we have

$$
\begin{aligned}
&\left(1+\sigma_1^2\beta\right)\|\boldsymbol{U}^{n+1}\|_\infty\\
=&\|\frac{\sigma_1^2}{2}\beta\left(u_{1,m-1}^{n+1}+u_{1,m+1}^{n+1}\right) + u_{1,m}^n + \alpha_{12}\Delta\tau e^{((\xi_2-\xi_1)\tau_n+(\eta_2-\eta_1)x_m)}u_{2,m}^n\\
&+\lambda_1\Delta\tau\boldsymbol{R}_{1,m}^n + \frac{\lambda_1 C_1\Delta\tau\Delta x}{2}\boldsymbol{\Phi}_{1,m}^\top\boldsymbol{U}_1^n\|_\infty\\
\le&\sigma_1^2\beta\|\boldsymbol{U}^{n+1}\|_\infty + \|\boldsymbol{U}^n\|_\infty + \alpha_{12}\Delta\tau e^{((\xi_2-\xi_1)\tau_n+(\eta_2-\eta_1)x_m)}\|\boldsymbol{U}^n\|_\infty\\
&+\lambda_1\Delta\tau\boldsymbol{R}_{1,m}^n + \lambda_1\Delta\tau\|\frac{C_1\Delta x}{2}\boldsymbol{\Phi}_{1,m}^\top\boldsymbol{U}^n\|_\infty\\
\le&\sigma_1^2\beta\|\boldsymbol{U}^{n+1}\|_\infty + \|\boldsymbol{U}^n\|_\infty + C^*\Delta\tau\|\boldsymbol{U}^n\|_\infty\\
&+\lambda_1\Delta\tau\boldsymbol{R}_{1,m}^n + \lambda_1\Delta\tau\|\frac{C_1\Delta x}{2}\boldsymbol{\Phi}_{1,m}^\top\boldsymbol{U}^n\|_\infty,
\end{aligned}
\tag{27}
$$

where C^* is a constant that only depends on the bounded solving domain and satisfies

$$
|\alpha_{i,3-i}e^{((\xi_{3-i}-\xi_i)\tau_n+(\eta_{3-i}-\eta_i)x_m)}| \le C^*, \quad i=1,2.
$$

For the fourth term on the right of the inequality (27), by using the property of the probability density function $g(y)$, we have

$$
\begin{aligned}
\boldsymbol{R}_{i,j}^n &\le \sup_{y\in(0,e^{-L-x_j}]}|w_i^*(x_j+\ln y,\tau_n)y^{\eta_i}|\int_0^{e^{-L-x_j}} g(y)\mathrm{d}y\\
&\le \|\boldsymbol{U}^n\|_\infty \sup_{y\in(0,e^{-L-x_j}]}|y^{\eta_i}|\\
&\le I^*\|\boldsymbol{U}^n\|_\infty,
\end{aligned}
$$

where $I^* = \max\{e^{-2\eta_1 L}, e^{-2\eta_2 L}, 1\}$. Now, we deal with the last term on the right of the inequality (27). Because all the elements of the vector $\boldsymbol{\Phi}_{i,j}$ are positive, let

$$M_\Phi = \max_{0\le j\le N_x} \left\{ \max\left(\frac{C_1\Delta x}{2}\boldsymbol{\Phi}_{1,j}^\top, \frac{C_2\Delta x}{2}\boldsymbol{\Phi}_{2,j}^\top \right) \right\},$$

then we could get

$$\|\frac{C_1\Delta x}{2}\boldsymbol{\Phi}_{1,m}^\top \boldsymbol{U}^n\|_\infty \le M_\Phi \|\boldsymbol{U}^n\|_\infty.$$

Therefore, according to above scalings, it has

$$\|\boldsymbol{U}^{n+1}\|_\infty \le (1 + H\Delta\tau)\,\|\boldsymbol{U}^n\|_\infty. \tag{28}$$

Here, $H = C^* + (M_\Phi + I^*)\max\{\lambda_1, \lambda_2\}$.

Further, combining (26) and (28), we have

$$\|\boldsymbol{U}^{n+1}\|_\infty \le \max\{e^{-\xi^*\Delta\tau}, (1 + H\Delta\tau)\}\|\boldsymbol{U}^n\|_\infty,$$

which yields

$$\begin{aligned}\|\boldsymbol{U}^{n+1}\|_\infty &\le \left(\max\{e^{-\xi^*\Delta\tau}, (1 + H\Delta\tau)\}\right)^{n+1}\|\boldsymbol{U}^0\|_\infty \\ &= \max\{e^{-\xi^*(n+1)\Delta\tau}, (1 + H\Delta\tau)^{n+1}\}\|\boldsymbol{U}^0\|_\infty.\end{aligned}$$

According to Bernoulli inequality, we know that

$$\begin{aligned}\max\{e^{-\xi^*(n+1)\Delta\tau}, (1 + H\Delta\tau)^{n+1}\} &\le \max\left\{ e^{-\xi^* T}, \lim_{n\to+\infty}\left(1 + \frac{HT}{n+1}\right)^{n+1} \right\} \\ &= \max\{e^{-\xi^* T}, e^{HT}\}.\end{aligned}$$

Finally, let $C = \max\{e^{-\xi^* T}, e^{HT}\}$, we could get the estimation (25). $\square$

Next, we begin our analysis of the monotonicity with the following notations. Let

$$\varphi_j\left(u_{i,j}^{n+1}, u_{i,j-1}^{n+1}, u_{i,j+1}^{n+1}, \boldsymbol{U}^n\right) = a u_{i,j}^{n+1} - b u_{i,j-1}^{n+1} - b u_{i,j+1}^{n+1} - F_j\left(\boldsymbol{U}^n\right), \quad 1 \le j \le N_x - 1,$$

where $a = 1 + \sigma_i^2\beta$, $b = \sigma_i^2\beta/2$, and

$$F_j\left(\boldsymbol{U}^n\right) = \frac{\lambda_i\Delta\tau C_i\Delta x}{2}\boldsymbol{\Phi}_{i,j}^\top\boldsymbol{U}_i^n + u_{i,j}^n + \alpha_{i,3-i}\Delta\tau e^{(\eta_{3-i}-\eta_i)x_j + (\xi_{3-i}-\xi_i)\tau_n} u_{3-i,j}^n + \lambda_i\Delta\tau\boldsymbol{R}_{i,j}^n.$$

For any $j = 1, \cdots, N_x - 1$, defining

$$\psi_j\left(u_{i,j}^{n+1}, u_{i,j-1}^{n+1}, u_{i,j+1}^{n+1}, \boldsymbol{U}^n\right) = \min\left(\varphi_j\left(u_{i,j}^{n+1}, u_{i,j-1}^{n+1}, u_{i,j+1}^{n+1}, \boldsymbol{U}^n\right), u_{i,j}^{n+1} - u_{i,j}^{n+1,*}\right),$$

we can reformulate the discretization scheme in (21) into the form of

$$\psi_j\left(u_{i,j}^{n+1}, u_{i,j-1}^{n+1}, u_{i,j+1}^{n+1}, \boldsymbol{U}^n\right) = 0, \quad j = 1, \cdots, N_x - 1, \tag{29}$$

and deduce the following result.

Theorem 3. *The discretization scheme in (29) is monotone and independent of the partitions $\{J_\tau\}$ and $\{I_h\}$ in (17), namely, it holds that*

$$\begin{aligned}&\psi_j\left(u_{i,j}^{n+1}, u_{i,j-1}^{n+1} + \varepsilon_1, u_{i,j+1}^{n+1} + \varepsilon_2, \boldsymbol{U}^n + \varepsilon_3\boldsymbol{e}_{2(N_x+1)}\right) \\ \le&\psi_j\left(u_{i,j}^{n+1}, u_{i,j-1}^{n+1}, u_{i,j+1}^{n+1}, \boldsymbol{U}^n\right), \quad \forall\varepsilon_1 \ge 0, \quad \varepsilon_2 \ge 0, \quad \varepsilon_3 \ge 0; \\ &\psi_j\left(u_{i,j}^{n+1} + \varepsilon, u_{i,j-1}^{n+1}, u_{i,j+1}^{n+1}, \boldsymbol{U}^n\right) \\ \ge&\psi_j\left(u_{i,j}^{n+1}, u_{i,j-1}^{n+1}, u_{i,j+1}^{n+1}, \boldsymbol{U}^n\right), \quad \forall\varepsilon \ge 0,\end{aligned}$$

where $\boldsymbol{e}$ denotes the vector where all the entries are ones.

Proof. For any $\varepsilon_1 \geq 0, \varepsilon_2 \geq 0, \varepsilon_3 \geq 0$, we have

$$\begin{aligned}
&\varphi_j\left(u_{i,j}^{n+1}, u_{i,j-1}^{n+1}+\varepsilon_1, u_{i,j+1}^{n+1}+\varepsilon_2, \boldsymbol{U}^n+\varepsilon_3 \boldsymbol{e}_{2(N_x+1)}\right) \\
=&\varphi_j\left(u_{i,j}^{n+1}, u_{i,j-1}^{n+1}, u_{i,j+1}^{n+1}, \boldsymbol{U}^n\right)-b\varepsilon_1-b\varepsilon_2 \\
&-\frac{\lambda_i \Delta\tau C_i \Delta x}{2} \boldsymbol{\Phi}_{i,j}^{\top} \boldsymbol{e}_{N_x+1}\varepsilon_3-(1+\alpha_{il}\Delta\tau e^{(\eta_l-\eta_i)x_j+(\xi_l-\xi_i)\tau_n})\varepsilon_3 \\
\leq&\varphi_j\left(u_{i,j}^{n+1}, u_{i,j-1}^{n+1}, u_{i,j+1}^{n+1}, \boldsymbol{U}^n\right),
\end{aligned}$$

According to the definition of ψ_j, we have

$$\psi_j\left(u_{i,j}^{n+1}, u_{i,j-1}^{n+1}+\varepsilon_1, u_{i,j+1}^{n+1}+\varepsilon_2, \boldsymbol{U}^n+\varepsilon_3 \boldsymbol{e}_{2(N_x+1)}\right) \leq \psi_j\left(u_{i,j}^{n+1}, u_{i,j-1}^{n+1}, u_{i,j+1}^{n+1}, \boldsymbol{U}^n\right).$$

In addition, by using the nonnegative complementarity condition in (21), for any $\varepsilon \geq 0$, it has

$$\begin{aligned}
&\psi_j\left(u_{i,j}^{n+1}+\varepsilon, u_{i,j-1}^{n+1}, u_{i,j+1}^{n+1}, \boldsymbol{U}^n\right) \\
=&\min\left(\varphi_j\left(u_{i,j}^{n+1}, u_{i,j-1}^{n+1}, u_{i,j+1}^{n+1}, \boldsymbol{U}^n\right)+a\varepsilon, u_{i,j}^{n+1}+\varepsilon-u_{i,j}^{n+1,*}\right) \\
\geq&\min\left(\varphi_j\left(u_{i,j}^{n+1}, u_{i,j-1}^{n+1}, u_{i,j+1}^{n+1}, \boldsymbol{U}^n\right), u_{i,j}^{n+1}-u_{i,j}^{n+1,*}\right) \\
=&\psi_j\left(u_{i,j}^{n+1}, u_{i,j-1}^{n+1}, u_{i,j+1}^{n+1}, \boldsymbol{U}^n\right).
\end{aligned}$$

The proof of monotonicity is completed. □

At the end of this subsection, we present the consistency of the discretization scheme by the following result.

Theorem 4. *Suppose that the probability density function $g(y)$ in (2) is continuous almost everywhere (regardless of the set of all partition points). Then the discretization scheme defined in (22) is consistent with the theoretical operator $\mathscr{L}_i$ for $i = 1, 2$, which means the numerical scheme (21) is consistent with the continuous model (15). Moreover, if $g(y)$ is twice continuously differentiable almost everywhere (regardless of the set of all partition points), then the truncation error will be $\mathcal{O}(\Delta\tau + \Delta x^2)$ pointwisely.*

Proof. The truncation error $\boldsymbol{\Upsilon}_{i,j}^{n+1}$ of the difference scheme (22) is given by:

$$\begin{aligned}
\boldsymbol{\Upsilon}_{i,j}^{n+1} =&\boldsymbol{L}_i w_{i,j}^{n+1}-\mathscr{L}_i w_i(x_j,\tau_{n+1}) \\
=&-\lambda_i\left(\frac{C_i\Delta x}{2}\boldsymbol{\Phi}_{i,j}^{\top}\boldsymbol{W}_i^n+\boldsymbol{R}_{i,j}^n\right)+\frac{1}{\Delta\tau}(w_{i,j}^{n+1}-w_{i,j}^n-\frac{1}{2}\sigma_i^2\beta\delta_x^2 w_{i,j}^{n+1} \\
&-\Delta\tau\alpha_{il}w_{l,j}^n e^{((\xi_l-\xi_i)\tau_n+(\eta_l-\eta_i)x_j)})-\mathscr{L}_i w_i(x_j,\tau_{n+1}), \quad l=3-i,
\end{aligned} \tag{30}$$

where $\boldsymbol{W}_i^n = \left(w_{i,0}^n, w_{i,1}^n, \ldots, w_{i,N_x}^n\right)^{\top}$ and $\delta_x^2 w_{i,j}^{n+1} = w_{i,j+1}^{n+1} - 2w_{i,j}^{n+1} + w_{i,j-1}^{n+1}$. From Theorem 3.2 of [14], the solution of problem (15) is continuously differentiable in temporal direction and twice continuously differentiable in spatial direction over the interior of the domain. Therefore, by Taylor expansion, we have

$$\begin{aligned}
\boldsymbol{\Upsilon}_{i,j}^{n+1} =& \lambda_i \int_{-L-x_j}^{L-x_j} w_i\left(x_j+z,\tau_n\right) g\left(e^z\right) e^{(\eta_i+1)z}\mathrm{d}z-\lambda_i\frac{C_i\Delta x}{2}\boldsymbol{\Phi}_{i,j}^{\top}\boldsymbol{W}_i^n \\
&+\mathcal{O}\left(\Delta\tau\right)+\mathcal{O}\left(\Delta x^2\right).
\end{aligned} \tag{31}$$

which, in view of the continuity of $g(y)$, the consistency is meet by

$$\lim_{(\Delta\tau,\Delta x)\to(0,0)} \boldsymbol{\Upsilon}_{i,j}^{n+1} = 0.$$

Additionally, with the above observation, we can obtain that $\boldsymbol{\Upsilon}_{i,j}^{n+1} = \mathcal{O}(\Delta\tau + \Delta x^2)$ if $g(y)$ is twice continuously differentiable almost everywhere. □

Remark 5. We notice that the continuous problem (15) satisfies the strong comparison principle [14]. Thus the numerical scheme converges to the viscosity solution of the corresponding problem [5] by the stability, monotonicity, and consistency above.

3.3 Error Estimation

In this subsection, we will provide the error estimation of the discretization scheme grounded on the previous analysis in subsection 3.2. First, we deliver the equivalent variational inequality problems of problems (15) and (24) by some derivation and the available result, respectively, then state our result of the error estimation.

Lemma 4. *Let $V_{i,\tau}$ $(i=1,2)$ be the sets defined as*

$$V_{i,\tau}=\left\{v\in C^{2,1}:\quad \begin{array}{l} v(x,\tau)\geq w_i^*(x,\tau),\ \forall(x,\tau)\in(L,L)\times(0,T];\\ v(-L,\tau)=w_i^*(-L,\tau),\ v(L,\tau)=w_i^*(L,\tau),\ \forall\tau\in(0,T]\end{array}\right\},$$

then the problem (15) is equivalent to the following variational inequality problem,

Find $w_i\in V_{i,\tau}(i=1,2)$ such that for any $v\in V_{i,\tau}$,

$$\left\{\begin{array}{ll}\mathscr{L}_i w_i(x,\tau)\cdot(v(x,\tau)-w_i(x,\tau))\geq 0, & \forall\ (x,\tau)\in(-L,L)\times(0,T],\\ w_i(x,0)=w_i^*(x,0), & \forall\ x\in(-L,L).\end{array}\right. \tag{32}$$

Proof. For the necessity, let $w_i(i=1,2)$ be the solution to problem (15), then we can directly have $w_i\in V_{i,\tau}$ and $w_i(x,0)=w_i^*(x,0)$. If $w_i>w_i^*$ at (x,τ), then from complementarity condition in (15) we have $\mathscr{L}_i w_i(x,\tau)=0$, which yields the inequality in (32). If $w_i=w_i^*$ at (x,τ), then for any $v\in V_{i,\tau}$ we have $v-w_i\geq 0$ at (x,τ). Using the inequality $\mathscr{L}_i w_i(x,\tau)\geq 0$ in (15), we can get the inequality in (32).

On the other hand, if $w_i(i=1,2)$ is the solution to problem (32), then we only need to verify $\mathscr{L}_i w_i\geq 0$ and $\mathscr{L}_i w_i(w_i-w_i^*)=0$. Similarly, if $w_i>w_i^*$ at (x,τ), let $v=(w_i+w_i^*)/2$ and w_i^* successively, which directly yields $\mathscr{L}_i w_i(x,\tau)=0$ and the complementarity condition. If $w_i=w_i^*$ at (x,τ), then it is trivial to finish the proof by using the inequality in (32). □

Lemma 5 (cf. [11])**.** *LCP (24) is equivalent to the variational inequality problem*

$$\left\{\begin{array}{l}\left(\boldsymbol{B}\bar{\boldsymbol{U}}^{n+1}+\mathscr{F}\left(\bar{\boldsymbol{U}}^{n}\right),\boldsymbol{V}-\bar{\boldsymbol{U}}^{n+1}\right)\geq 0,\quad \forall\ \boldsymbol{V}\geq\bar{\boldsymbol{U}}^{n+1,*},\\ \bar{\boldsymbol{U}}^{0}=\bar{\boldsymbol{U}}^{0,*}.\end{array}\right. \tag{33}$$

Theorem 5. *Let $\{w_i(x,\tau),\ i=1,2\}$ and $\{\bar{\boldsymbol{U}}^n,\ n=0,1,\ldots,N_t\}$ be the solutions of problem (15) and problem (24), respectively. Then we can give the following error estimation in discrete L_2-norm:*

$$\begin{aligned}\left\|\bar{\boldsymbol{U}}^{N_t}-\bar{\boldsymbol{W}}^{N_t}\right\|_h&=\left(\sum_{j=1}^{N_x-1}\Delta x\left(\left|u_{1,j}^{N_t}-w_{1,j}^{N_t}\right|^2+\left|u_{2,j}^{N_t}-w_{2,j}^{N_t}\right|^2\right)\right)^{\frac{1}{2}}\\&=\mathcal{O}\left(\Delta\tau+\Delta x^2\right),\end{aligned} \tag{34}$$

where $\bar{\boldsymbol{W}}^n=(w_{1,1}^n,\ldots,w_{1,N_x-1}^n,w_{2,1}^n,\ldots,w_{2,N_x-1}^n)^\top$.

Proof. From Lemma 4 and the definition of truncation error in (30), it follows that

$$\left(\boldsymbol{B}\bar{\boldsymbol{W}}^{n+1}+\mathscr{F}\left(\bar{\boldsymbol{W}}^{n}\right)-\Delta\tau\boldsymbol{\Upsilon}^{n+1},\boldsymbol{V}-\bar{\boldsymbol{W}}^{n+1}\right)\geq 0,\quad\forall\ \boldsymbol{V}\geq\bar{\boldsymbol{U}}^{n+1,*}, \tag{35}$$

for $n=0,1,\ldots,N_t-1$, where $\boldsymbol{\Upsilon}^{n+1}=\left(\boldsymbol{\Upsilon}_{1,1}^{n+1},\ldots,\boldsymbol{\Upsilon}_{1,N_x-1}^{n+1},\boldsymbol{\Upsilon}_{2,1}^{n+1},\ldots,\boldsymbol{\Upsilon}_{1,N_x-1}^{n+1}\right)^{\top}$ and $\boldsymbol{\Upsilon}_{i,j}^{n+1}=\mathcal{O}(\Delta\tau+\Delta x^2)$, which has been proved in Theorem 4.

Let $\boldsymbol{\varepsilon}^{n+1}=\bar{\boldsymbol{W}}^{n+1}-\bar{\boldsymbol{U}}^{n+1}$. With $\boldsymbol{V}=\bar{\boldsymbol{W}}^{n+1}$ and $\boldsymbol{V}=\bar{\boldsymbol{U}}^{n+1}$ in (33) and (35), respectively, we can obtain that

$$\begin{aligned}
\left(\boldsymbol{B}\boldsymbol{\varepsilon}^{n+1},\boldsymbol{\varepsilon}^{n+1}\right)&=\left(\boldsymbol{B}\bar{\boldsymbol{W}}^{n+1},\bar{\boldsymbol{W}}^{n+1}-\bar{\boldsymbol{U}}^{n+1}\right)-\left(\boldsymbol{B}\bar{\boldsymbol{U}}^{n+1},\bar{\boldsymbol{W}}^{n+1}-\bar{\boldsymbol{U}}^{n+1}\right)\\
&\le\left(-\mathscr{F}\left(\bar{\boldsymbol{W}}^{n}\right)+\Delta\tau\boldsymbol{\Upsilon}^{n+1},\bar{\boldsymbol{W}}^{n+1}-\bar{\boldsymbol{U}}^{n+1}\right)-\left(-\mathscr{F}\left(\bar{\boldsymbol{U}}^{n}\right),\bar{\boldsymbol{W}}^{n+1}-\bar{\boldsymbol{U}}^{n+1}\right)\\
&=\left(\mathscr{F}\left(\bar{\boldsymbol{U}}^{n}\right)-\mathscr{F}\left(\bar{\boldsymbol{W}}^{n}\right)+\Delta\tau\boldsymbol{\Upsilon}^{n+1},\bar{\boldsymbol{W}}^{n+1}-\bar{\boldsymbol{U}}^{n+1}\right)\\
&=\left(\left(-\boldsymbol{A}+\Delta\tau\boldsymbol{\Phi}\right)\boldsymbol{\varepsilon}^{n}+\Delta\tau\boldsymbol{\Upsilon}^{n+1},\boldsymbol{\varepsilon}^{n+1}\right)\\
&\le(1+\Delta\tau(D^*+R^*))\|\boldsymbol{\varepsilon}^{n}\|\|\boldsymbol{\varepsilon}^{n+1}\|+\Delta\tau\|\boldsymbol{\Upsilon}^{n+1}\|\|\boldsymbol{\varepsilon}^{n+1}\|,
\end{aligned}\tag{36}$$

where $D^*=\max\{|\alpha_{12}|,|\alpha_{21}|\}e^{L|\eta_2-\eta_1|+T|\xi_2-\xi_1|}$ and

$$R^*=\begin{cases}\max\{\lambda_1C_1,\lambda_2C_2\}\Delta x, & \text{(Merton's model)}\\ \max\{\lambda_1,\lambda_2\}\max\{q\theta_2,p\theta_1\}e^{2L(\max\{\theta_1,\theta_2\}+\max\{\eta_1,\eta_2\})}\Delta x, & \text{(Kou's model)}\end{cases}$$

Moreover, it holds that

$$\left(\boldsymbol{B}\boldsymbol{\varepsilon}^{n+1},\boldsymbol{\varepsilon}^{n+1}\right)\ge\lambda_{min}\|\boldsymbol{\varepsilon}^{n+1}\|^2,\tag{37}$$

where λ_{min} is the minimum eigenvalue of the positive definite matrix $\boldsymbol{B}$.

Combing the inequalities (36) and (37), let $G^*=D^*+R^*$, and we have

$$\begin{aligned}
\|\boldsymbol{\varepsilon}^{N_t}\|&\le\frac{1+G^*\Delta\tau}{\lambda_{min}}\|\boldsymbol{\varepsilon}^{N_t-1}\|+\frac{\Delta\tau}{\lambda_{min}}\|\boldsymbol{\Upsilon}^{N_t}\|\\
&\le\left(\frac{1+G^*\Delta\tau}{\lambda_{min}}\right)^{N_t}\|\boldsymbol{\varepsilon}^{0}\|+\left(\sum_{k=0}^{N_t-1}\left(\frac{1+G^*\Delta\tau}{\lambda_{min}}\right)^{k}\right)\frac{\Delta\tau}{\lambda_{min}}\|\boldsymbol{\Upsilon}^{N_t}\|\\
&=\left(\sum_{k=0}^{N_t-1}\left(\frac{1+G^*\Delta\tau}{\lambda_{min}}\right)^{k}\right)\frac{\Delta\tau}{\lambda_{min}}\|\boldsymbol{\Upsilon}^{N_t}\|.
\end{aligned}\tag{38}$$

Now, we are going to check the boundedness of the coefficient of the right-hand term in (38).

By the property of tridiagonal pseudo-Toeplitz matrices [26], all eigenvalues of the matrix $\boldsymbol{B}_i(i=1,2)$ can be expressed as

$$\lambda_k=1+\sigma_i^2\beta(1-\cos(k\pi/N_x)),\ k=1,\ldots,N_x-1,$$

and we can get

$$\lambda_{min}=1+\sigma_*^2\beta(1-\cos(\frac{\pi}{N_x}))=1+\sigma_*^2\Delta\tau(\frac{\pi^2}{8L^2}+o(\Delta x)),$$

with $\sigma_*=\max\{\sigma_1,\sigma_2\}$. If $(1+G^*\Delta\tau)/\lambda_{min}\ge1$, we have

$$\frac{T}{2}\le\left(\sum_{k=0}^{N_t-1}\left(\frac{1+G^*\Delta\tau}{\lambda_{min}}\right)^{k}\right)\frac{\Delta\tau}{\lambda_{min}}\le T\left(1+G^*\Delta\tau\right)^{N_t}\le Te^{G^*T},\tag{39}$$

otherwise,

$$Te^{-(\frac{\sigma_*^2\pi^2}{4L^2})T}\le\left(\sum_{k=0}^{N_t-1}\left(\frac{1+G^*\Delta\tau}{\lambda_{min}}\right)^{k}\right)\frac{\Delta\tau}{\lambda_{min}}\le T.\tag{40}$$

With the above observations, we can verify the desired boundedness, which completes the proof. □

4 Numerical Experiments

In this section, we report some numerical results to show the performance of the proposed scheme. We first specify the made-to-order projection and contraction method for solving the discretized problem (24), then verify the efficiency of our scheme. All the experiments are performed in MATLAB (version R2022a) on an Intel Core i7 CPU of 2.10 GHz.

4.1 Implementation with Projection and Contraction Method

To simplify the format of the algorithm, let $\widetilde{\boldsymbol{U}}^{n+1} = \bar{\boldsymbol{U}}^{n+1} - \bar{\boldsymbol{U}}^{n+1,*}$ and $\widetilde{\mathscr{F}}^{n+1} = \mathscr{F}(\bar{\boldsymbol{U}}^{n}) + \boldsymbol{B}\bar{\boldsymbol{U}}^{n+1,*}$, and the model (24) can be represented by a standard LCP:

$$\begin{cases} \left(\boldsymbol{B}\widetilde{\boldsymbol{U}}^{n+1} + \widetilde{\mathscr{F}}^{n+1}, \widetilde{\boldsymbol{U}}^{n+1}\right) = 0, \\ \boldsymbol{B}\widetilde{\boldsymbol{U}}^{n+1} + \widetilde{\mathscr{F}}^{n+1} \geq \boldsymbol{0}, \quad \widetilde{\boldsymbol{U}}^{n+1} \geq \boldsymbol{0}, \\ \widetilde{\boldsymbol{U}}^{0} = \boldsymbol{0}. \end{cases} \tag{41}$$

Following we shall introduce an efficient projection and contraction method (PCM, [20]) to solve the LCP (41).

Let $\Omega = \left\{\widetilde{\boldsymbol{U}}^{n+1} \in \mathbb{R}^{2(N_x-1)} \mid \widetilde{\boldsymbol{U}}^{n+1} \geqslant 0\right\}$, and define the projector $P_\Omega(\widetilde{\boldsymbol{U}}^{n+1})$ as follows

$$P_\Omega(\widetilde{\boldsymbol{U}}^{n+1}) = \arg\min_{v\in\Omega} \|\widetilde{\boldsymbol{U}}^{n+1} - v\|_2 = \max\{\widetilde{\boldsymbol{U}}^{n+1}, 0\}.$$

Then one can verify that solving the LCP (41) is equivalent to finding the zero point of the function

$$e(\widetilde{\boldsymbol{U}}^{n+1}) = \widetilde{\boldsymbol{U}}^{n+1} - P_\Omega\left[\widetilde{\boldsymbol{U}}^{n+1} - \left(\boldsymbol{B}\widetilde{\boldsymbol{U}}^{n+1} + \widetilde{\mathscr{F}}^{n+1}\right)\right].$$

Now, we introduce the framework of PCM to solve the above nonlinear equation as Algorithm 1.

Algorithm 1 Framework of PCM

```
Input: Ũ^n, F̃^{n+1},
Output: Ũ^{n+1}.
Let Ũ^(0) = Ũ^n,
for k = 0, 1, ... do
    if e(Ũ^(k)) ≠ 0 then
        d(Ũ^(k)) = (B^T + I) e(Ũ^(k)),
        ρ(Ũ^(k)) = ||e(Ũ^(k))||^2 / ||d(Ũ^(k))||^2,
        Ũ^(k+1) = Ũ^(k) − ρ(Ũ^(k)) d(Ũ^(k)).
    end if
    Ũ^{n+1} = Ũ^(k+1).
end for
```

Adding some acceleration skills to Algorithm 1, we can improve its efficiency and robustness. And we apply Algorithm 2 to solve the LCP (41) in practice.

Algorithm 2 Practical PCM

```
Input: Ũ^n, F̃^{n+1}, ν ∈ (0,1), μ ∈ (0,1), ϱ ∈ (1,2), ε = 10^{-9},
Output: Ũ^{n+1}.
Let k = 0, β^(0) = 1,
```

$\widetilde{\boldsymbol{U}} = \widetilde{\boldsymbol{U}}^n, \boldsymbol{F}_u = \boldsymbol{B}\widetilde{\boldsymbol{U}} + \widetilde{\mathscr{F}}^{n+1}$,
$tol = abs\left(\widetilde{\boldsymbol{U}} - \max\left(\widetilde{\boldsymbol{U}} - \boldsymbol{F}_u, 0\right)\right)$.
while $(tol > \varepsilon)$ **do**
    $\widetilde{\boldsymbol{U}}^{(k)} = \widetilde{\boldsymbol{U}}, \boldsymbol{F}_u^{(k)} = \boldsymbol{F}_u, \widetilde{\boldsymbol{U}} = \max\left(\widetilde{\boldsymbol{U}}^{(k)} - \beta^{(k)}\boldsymbol{F}_u^{(k)}, 0\right)$,
    $\boldsymbol{F}_u = \boldsymbol{B}\widetilde{\boldsymbol{U}} + \widetilde{\mathscr{F}}^{n+1}$,
    $\boldsymbol{d}_u = \widetilde{\boldsymbol{U}}^{(k)} - \widetilde{\boldsymbol{U}}, \boldsymbol{d}_F = \beta^{(k)}\left(\boldsymbol{F}_u^{(k)} - \boldsymbol{F}_u\right), \rho^{(k)} = \|\boldsymbol{d}_F\| / \|\boldsymbol{d}_u\|$.
    while $(\rho^{(k)} > \nu)$ **do**
        $\beta^{(k)} = \frac{2}{3}\beta^{(k)} \min\left(1, 1/\rho^{(k)}\right), \widetilde{\boldsymbol{U}} = \max\left(\widetilde{\boldsymbol{U}}^{(k)} - \beta^{(k)}\boldsymbol{F}_u^{(k)}, 0\right)$,
        $\boldsymbol{F}_u = \boldsymbol{B}\widetilde{\boldsymbol{U}} + \widetilde{\mathscr{F}}^{n+1}$,
        $\boldsymbol{d}_u = \widetilde{\boldsymbol{U}}^{(k)} - \widetilde{\boldsymbol{U}}, \boldsymbol{d}_F = \beta^{(k)}\left(\boldsymbol{F}_u^{(k)} - \boldsymbol{F}_u\right), \rho^{(k)} = \|\boldsymbol{d}_F\| / \|\boldsymbol{d}_u\|$.
    end while
    $\boldsymbol{d}_{uF} = \boldsymbol{d}_u + \boldsymbol{d}_F, \nu_1 = \boldsymbol{d}_u^\top \boldsymbol{d}_u, \nu_2 = \boldsymbol{d}_{uF}^\top \boldsymbol{d}_{uF},\ \alpha^* = \nu_1/\nu_2$,
    $\widetilde{\boldsymbol{U}} = \widetilde{\boldsymbol{U}}^{(k)} - \alpha^* \varrho \boldsymbol{d}_{uF}, \boldsymbol{F}_u = \boldsymbol{B}\widetilde{\boldsymbol{U}} + \widetilde{\mathscr{F}}^{n+1}$,
    $tol = abs\left(\widetilde{\boldsymbol{U}} - \max\left(\widetilde{\boldsymbol{U}} - \boldsymbol{F}_u, 0\right)\right)$.
    if $(\rho^{(k)} < \mu)$ **then**
        $\beta^{(k)} = \beta^{(k)} * \varrho$.
    end if
    $k = k + 1$ and $\beta^{(k)} = \beta^{(k-1)}$.
end while
Let $\widetilde{\boldsymbol{U}}^{n+1} = \widetilde{\boldsymbol{U}}$.

We now bring some details of implementing Algorithm 2. Recall the matrix-vector form (23) in subsection 3.1, the computation of the approximate integral $\boldsymbol{\Phi}_i \bar{\boldsymbol{U}}_i^n$ usually requires $\mathcal{O}\left(N^2\right)$ operations. However, after observing $\boldsymbol{\Phi}_i$ is a Toeplitz matrix and converting the matrix-vector multiplication into a fast Fourier transformation form [2], the operations could be reduced to $\mathcal{O}\left(N \log N\right)$ in the case that N is the power of 2. Unfortunately, in our regime-switching model the degree of freedom N will always be in a form of $2k - 1$ where k is an integer, and we find that there is almost no difference between employing this trick and directly computing the matrix-vector multiplication in MATLAB.

4.2 Numerical Examples

In this part, we first demonstrate the effectiveness of our method (Finite Difference with Projection and Contraction Method: FDPCM) with the Radial Basis Collocation Method (RBCM) [6] as an indicator, and give 3-D plots of the option prices. Then we illustrate the results in Theorem 1 and verify the convergence order in Theorem 5. Finally, we show the efficiency of our method by making a comparison with RBCM.

We consider an one-year ($T = 1$) American put option under regime-switching jump-diffusion models and give two numerical examples as follows:

- Example 1 (Merton's model):

$$\sigma = \begin{pmatrix} 0.8 \\ 0.3 \end{pmatrix}, r = \begin{pmatrix} 0.05 \\ 0.05 \end{pmatrix}, d = \begin{pmatrix} 0.025 \\ 0.025 \end{pmatrix}, \lambda = \begin{pmatrix} 0.25 \\ 0.20 \end{pmatrix}, K = 1,$$

$$\mu = -0.025, \quad \delta = \sqrt{0.05}, \quad \mathcal{A} = \begin{pmatrix} -2 & 2 \\ 3 & -3 \end{pmatrix},$$

$$L = 2.0747.$$

- Example 2 (Kou's model):

$$\sigma = \begin{pmatrix} 0.8 \\ 0.3 \end{pmatrix}, r = \begin{pmatrix} 0.05 \\ 0.05 \end{pmatrix}, d = \begin{pmatrix} 0.025 \\ 0.025 \end{pmatrix}, \lambda = \begin{pmatrix} 0.25 \\ 0.20 \end{pmatrix}, K = 1,$$
$$\theta_1 = 3.0465, \quad \theta_2 = 3.0775, \quad p = 0.3445, \quad \mathcal{A} = \begin{pmatrix} -2 & 2 \\ 3 & -3 \end{pmatrix},$$
$$L = 2.1188.$$

Besides, the parameters in Algorithm 2 are set as $\nu = 0.9$, $\mu = 0.4$, $\rho = 1.5$, $\varepsilon = 10^{-8}$. Since the effectiveness of RBCM has been shown in [6], we compare our method FDPCM with it under the same spatial and temporal partition ($N_x = 256$, $N_t = 500$).

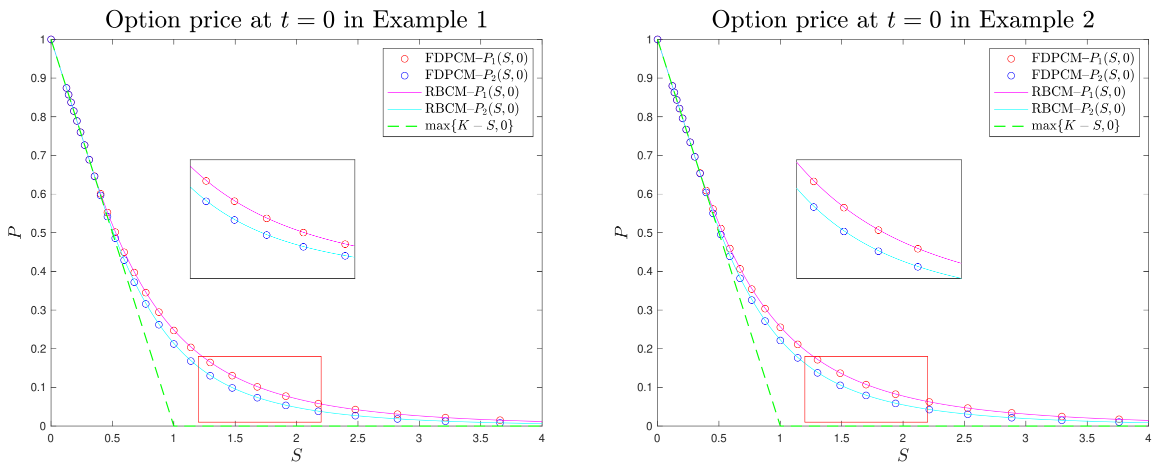

Figure 1: The option prices $P_i(S, 0)$ $(i = 1, 2)$ in Example 1 and Example 2.

The result from Figure 1 shows that the gap between the solutions of option prices at $t = 0$ by FDPCM and RBCM is acceptable in either Example 1 or Example 2, which means that FDPCM is a feasible method to solve the option pricing problem. Figures 2 and 3 show the 3-D plots of option prices in Example 1 and Example 2, respectively.

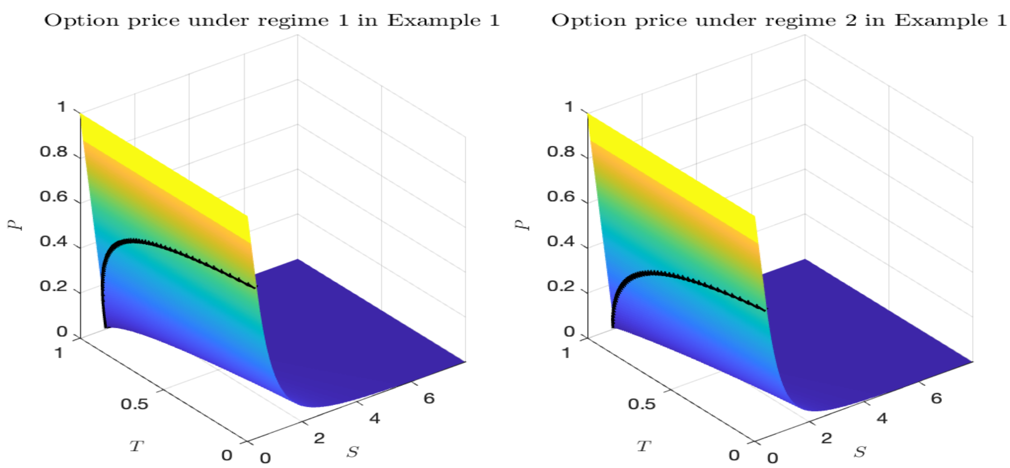

Figure 2: The option prices $P_i(S, 0)$ $(i = 1, 2)$ for Example 1.

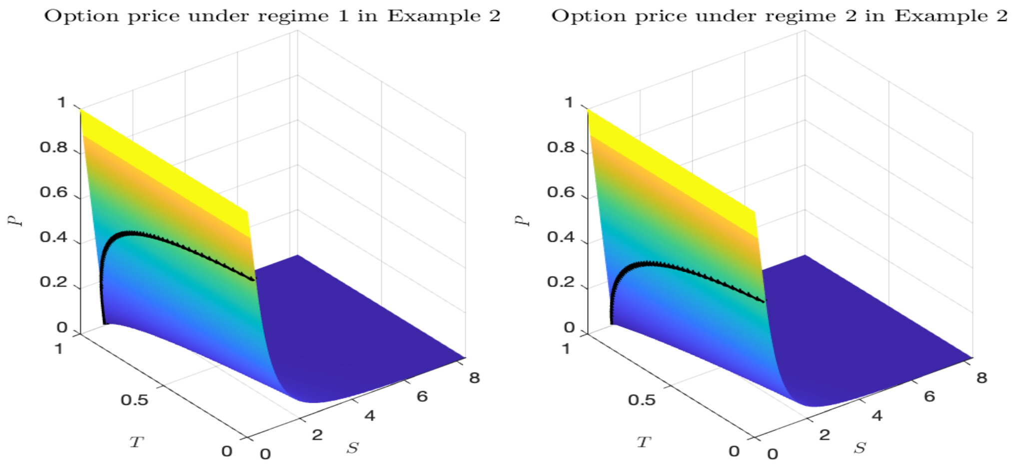

Figure 3: The option prices $P_i(S, 0)$ $(i = 1, 2)$ for Example 2.

Also, we present the optimal exercise boundaries of the two concerned examples in Figure 4. The numerical results visually illustrate the inequality in Theorem 1.

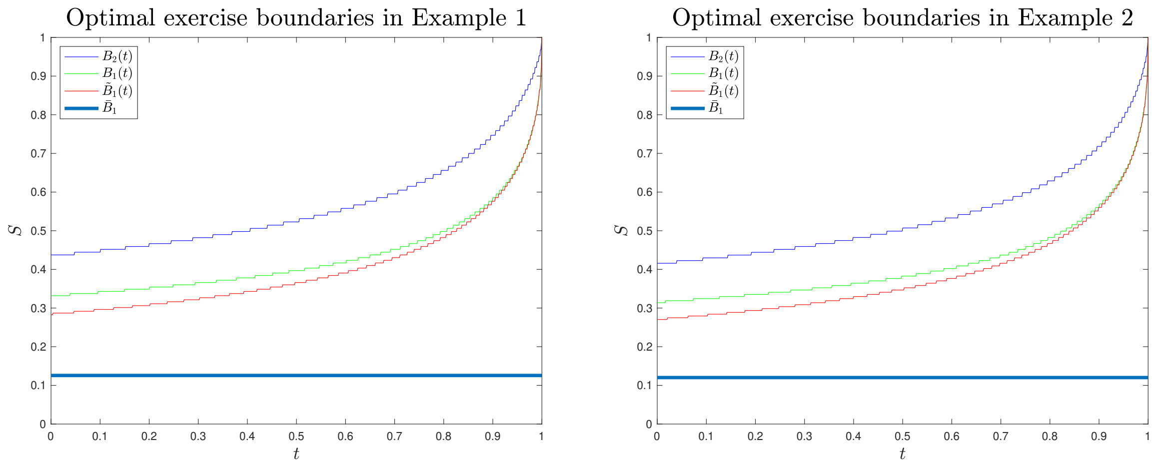

Figure 4: Optimal exercise boundaries stated in Theorem 1 for Example 1 and Example 2.

Next, we check the convergence order of our methods. As there is no closed-form solution for American put options under regime-switching jump-diffusion models, we use the numerical results obtained by FDPCM with an adequately fine mesh as the benchmarks where the mesh ratio $(\Delta x)^2/\Delta t$ is fixed at 0.8. Thus, for Example 1, we choose $N_x = 1024, N_t = 48720$; for Example 2, we choose $N_x = 1024, N_t = 46716$. First, we verify the convergence order in the spatial direction and fix $N_t = 48720$ and $N_t = 46716$ in Example 1 and 2 respectively to reduce the influence from the temporal direction. Figure 5 shows that the convergence order in the spatial direction is of order 2, which matches our estimation in Theorem 5. Further, we verify the convergence order in the temporal direction and fix $N_x = 1024$ to reduce the influence from the spatial direction. Figure 6 shows that the convergence order in the spatial direction is of order 1, which also matches our estimation in Theorem 5. It should be mentioned that we translated the data of log(error) of regime 2 for clarity in

Figure 5 and Figure 6.

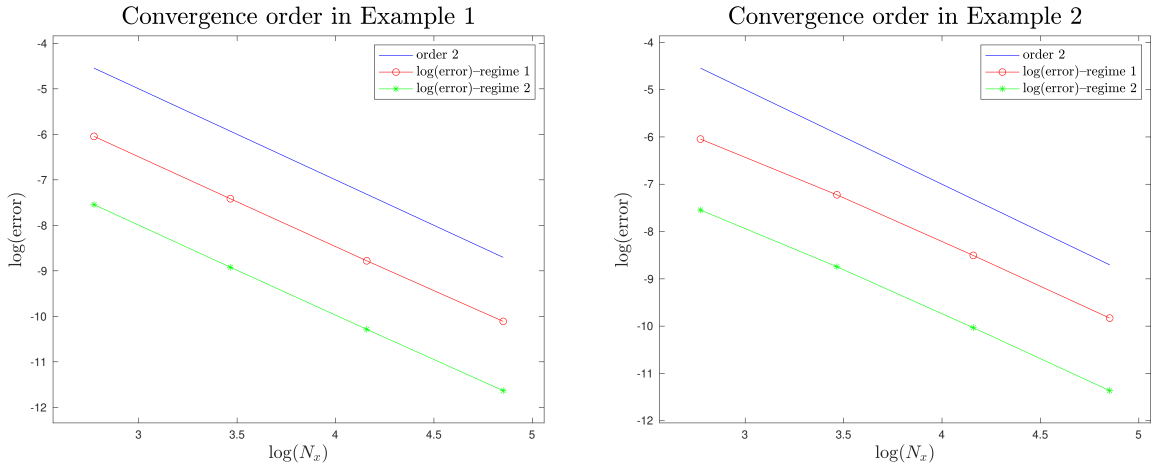

Figure 5: Convergence order in spatial direction under Example 1 and Example 2.

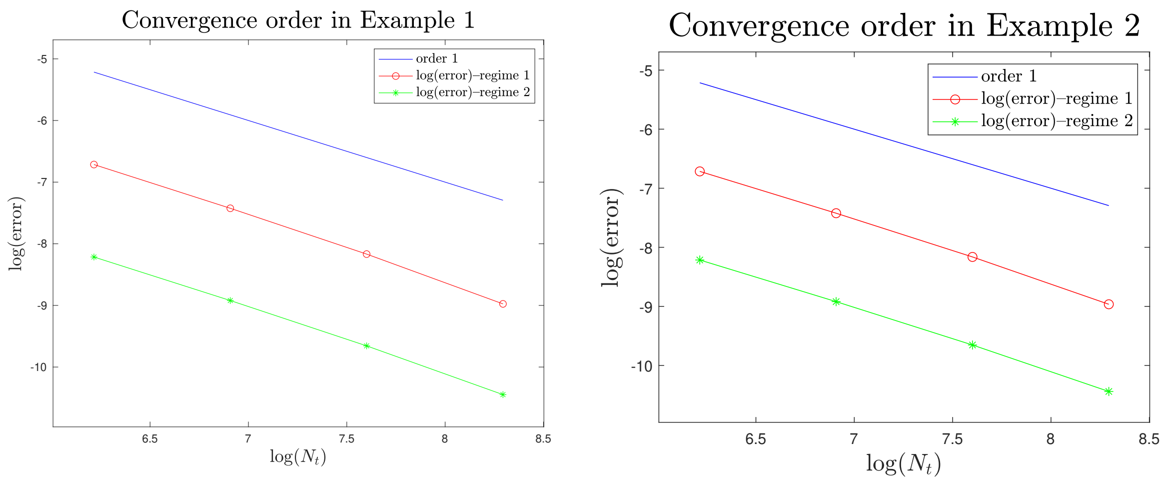

Figure 6: Convergence order in temporal direction under Example 1 and Example 2.

The last experiment devotes to verifying the efficiency of our method. We compare the error and running time of FDPCM and RBCM with the same partition (still fix the mesh ratio $(\Delta x)^2/\Delta t = 0.8$). Specifically, we use discrete L_2-norm defined in Theorem 5 for computing the error. The results in Table 1 indicate that our FDPCM is more competitive than RBCM.

Table 1: The errors of $\boldsymbol{P}(S,0)$ and computational costs for FDPCM and RBCM.

Example	N_x		N_t		Error (10^{-4})		Time (s)	
	FDPCM	RBCM	FDPCM	RBCM	FDPCM	RBCM	FDPCM	RBCM
1	256	256	3045	3045	3.25	5.82	11.12	17.35
2	256	256	2920	2920	4.22	4.63	9.88	20.50

5 Conclusions

This paper proposes an efficient numerical method for evaluating American options under regime-switching jump-diffusion models. By the relation of optimal exercise boundaries among several options, a simplified model defined on a bounded domain is first presented to approximate the original model defined on an unbounded domain. Then a composite trapezoidal formula and a finite difference method are applied to discretize the simplified model to be an LCP in finite dimensional space. Sequentially, we established the stability, monotonicity, consistency, and error estimation of the numerical scheme. Furthermore, based on the characteristics of the discretized matrix, a projection and contraction method is proposed to solve the LCP. Finally, several numerical simulations are carried out to verify the proposed method's theoretical analysis and efficiency.

Acknowledgments

This work was supported by the National Key Research and Development Program of China under the grant No.2020YFA0713602, the Education Department Project of Jilin Province under the grant No.JJKH20211031KJ, the NSF of Jilin Province under the grant No.20200201269JC, the SSF of Jilin Province under the grant No. 2020C026, and the Fundamental Research Funds for the Central Universities.

References

[1] Y. Achdou and O. Pironneau. *Computational Methods for Option Pricing.* SIAM, Philadelphia, 2005.

[2] A. Almendral and C. Oosterlee. Numerical valuation of options with jumps in the underlying. *Appl. Numer. Math.*, 53:1–18, 2005.

[3] U. Ascher, S. Ruuth, and B. Wetton. Implicit-explicit methods for time-dependent partial differential equations. *SIAM J. Numer. Anal.*, 32:797–823, 1995.

[4] L. Bachelier. Théorie de la spéculation. *Ann. Sci. Ec. Norm. Super.*, 17:21–86, 1900.

[5] G. Barles, C. Daher, and M. Romano. Convergence of numerical schemes for parabolic equations arising in finance theory. *Math. Models Methods Appl. Sci.*, 5:125–143, 1995.

[6] A. Bastani, Z. Ahmadi, and D. Damircheli. A radial basis collocation method for pricing american options under regime-switching jump-diffusion models. *Appl. Numer. Math.*, 65:79–90, 2013.

[7] F. Black and M. Scholes. The pricing of options and corporate liabilities. *J. Political Econ.*, 81:637–654, 1973.

[8] J. Buffington and R. Elliott. American options with regime switching. *Int. J. Theor. Appl. Finance*, 5:497–514, 2002.

[9] C. Chiarella, B. Kang, G. Meyer, and A. Ziogas. The evaluation of american option prices under stochastic volatility and jump-diffusion dynamics using the method of lines. *Int. J. Theor. Appl. Finance*, 12:393–425, 2009.

[10] R. Cont and E. Voltchkova. A finite difference scheme for option pricing in jump diffusion and exponential Lévy models. *SIAM J. Numer. Anal.*, 43:1596–1626, 2005.

[11] R. Cottle, J. Pang, and R. Stone. *The Linear Complementarity Problem.* SIAM, 2009.

[12] J. Cox, S. Ross, and M. Rubinstein. Option pricing: a simplified approach. *J. Financ. Econ.*, 7:229–263, 1979.

[13] M. Dai, Q. Zhang, and Q. Zhu. Trend following trading under a regime switching model. *SIAM J. Financial Math.*, 1:780–810, 2010.

[14] I. Florescu, R. Liu, and M. Mariani. Solutions to a partial integro-differential parabolic system arising in the pricing of financial options in regime-switching jump diffusion models. *Electron. J. Differ. Equ.*, 2012:1–12, 2012.

[15] J. Frank, H. Willem, and J. Verwer. On the stability of implicit-explicit linear multistep methods. *Appl. Numer. Math.*, 25:193–205, 1997.

[16] N. Haldrup and M. Nielsen. A regime switching long memory model for electricity prices. *J. Econom.*, 135:349–376, 2006.

[17] J. Hamilton. A new approach to the economic analysis of nonstationary time series and the business cycle. *Econometrica*, pages 357–384, 1989.

[18] H. Han and X. Wu. A fast numerical method for the Black–Scholes equation of american options. *SIAM J. Numer. Anal.*, 41:2081–2095, 2003.

[19] M. Hardy. A regime-switching model of long-term stock returns. *N. Am. Actuar. J.*, 5:41–53, 2001.

[20] B. He. A new method for a class of linear variational inequalities. *Math. Program.*, 66:137–144, 1994.

[21] A. Holmes and H. Yang. A front-fixing finite element method for the valuation of american options. *SIAM J. Sci. Comput.*, 30:2158–2180, 2008.

[22] L. Jiang. *Mathematical Modeling and Methods of Option Pricing.* World Scientific Publishing, Singapore, 2005.

[23] K. Kazmi. An IMEX predictor-corrector method for pricing options under regime-switching jump-diffusion models. *Int. J. Comput. Math.*, 96:1137–1157, 2019.

[24] A. Khaliq and R. Liu. New numerical scheme for pricing american option with regime-switching. *Int. J. Theor. Appl. Finance*, 12:319–340, 2009.

[25] S. Kou. A jump-diffusion model for option pricing. *Manage Sci.*, 48:1086–1101, 2002.

[26] D. Kulkarni, D. Schmidt, and S. Tsui. Eigenvalues of tridiagonal pseudo-Toeplitz matrices. *Linear Algebra Its Appl.*, 297:63–80, 1999.

[27] Y. Lee. Financial options pricing with regime-switching jump-diffusions. *Comput. Math. with Appl.*, 68:392–404, 2014.

[28] R. Merton. Option pricing when underlying stock returns are discontinuous. *J. Financ. Econ.*, 3:125–144, 1976.

[29] K. Patel and M. Mehra. Fourth-order compact finite difference scheme for american option pricing under regime-switching jump-diffusion models. *Int. J. Appl. Math.*, 3:547–567, 2017.

[30] H. Pham. Optimal stopping, free boundary, and american option in a jump-diffusion model. *Appl. Math. Optim.*, 35:145–164, 1997.

[31] N. Rambeerich and A. Pantelous. A high order finite element scheme for pricing options under regime switching jump diffusion processes. *J. Comput. Appl. Math.*, 300:83–96, 2016.

[32] M. Shirzadi, M. Rostami, M. Dehghan, and X. Li. American options pricing under regime-switching jump-diffusion models with meshfree finite point method. *Chaos Solitons Fractals*, 166:112919, 2023.

[33] H. Song, J. Xu, J. Yang, and Y. Li. Projection and contraction method for the valuation of american options under regime switching. *Commun. Nonlinear Sci. Numer. Simul.*, 109:106332, 2022.

[34] G. Tour, N. Thakoor, J. Ma, and D. Tangman. A spectral element method for option pricing under regime-switching with jumps. *J. Sci. Comput.*, 83:1–31, 2020.

[35] M. Yousuf, A. Khaliq, and S. Alrabeei. Solving complex PIDE systems for pricing american option under multi-state regime switching jump-diffusion model. *Comput. Math. with Appl.*, 75:2989–3001, 2018.

[36] K. Zhang, K. Teo, and M. Swartz. A robust numerical scheme for pricing american options under regime switching based on penalty method. *Comput. Econ.*, 43:463–483, 2014.

[37] Q. Zhang and X. Zhou. Valuation of stock loans with regime switching. *SIAM J. Control Optim.*, 48:1229–1250, 2009.